European Journal of Operational Research 315 (2024) 102–119

Contents lists available at ScienceDirect

European Journal of Operational Research

journal homepage: www.elsevier.com/locate/eor

Production, manufacturing, transportation and logistics

Network design with route planning for battery electric high-speed passenger vessel services

Håkon Furnes Havre [a], Ulrik Lien [a], Mattias Myklebust Ness [a], Kjetil Fagerholt [a,*], Kenneth Løvold Rødseth [b]

[a] Department of Industrial Economics and Technology Management, Norwegian University of Science and Technology, Trondheim, Norway
[b] Institute of Transport Economics, Oslo, Norway

ARTICLE INFO

Keywords:
Transportation
Routing and scheduling
Zero emissions
Passenger vessels

ABSTRACT

This paper studies the Zero Emission passenger Vessel Service Network Design Problem (ZEVSNDP) in order to investigate how technical and economic challenges related to diffusion of battery electric vessels can be alleviated by appropriate planning of services. The ZEVSNDP considers decisions that are strategic (i.e., vessel fleet and charging locations), tactical (i.e., routes, whether to omit servicing ports, fleet deployment, and operating frequencies), as well as operational (i.e., passenger flow, sailing speeds, and scheduling decisions). A novel Mixed Integer Programming (MIP) model considering operator and passenger costs is proposed for the ZEVSNDP. Since the MIP model cannot be solved to optimality by a commercial solver except for tiny instances, we implement a heuristic Decomposition Based (DB) solution method. The DB solution method is applied to a real complex passenger vessel service in Florø, Norway, as well as two other test instances focusing on short-range transport and dense markets, respectively. Except for the short-range test instance, abatement costs (i.e., the costs of removing CO_2 emissions by introducing battery electric vessels) are found to be significant. This is attributed to limited reach and time used for charging of battery electric vessels. Routes should consequently accommodate range limitations: omitting ports from the current route can be a cost-effective strategy when the cost of alternative transport for the passengers is moderate.

1. Introduction

Maritime transports constitute a non-negligible source of greenhouse gas emissions. Estimates suggest they were responsible for about three percent of global carbon dioxide (CO_2) emissions in 2018 (IMO, 2020) and about 3–4 percent of the European Union's CO_2 emissions in 2019 (EU, 2021). With anticipated growth in maritime activities, a transformation of the maritime sector is required to meet climate goals set by the International Maritime Organization (IMO) following the Paris agreement.

The Norwegian Government's Climate Plan 2021–2030 aims to halve domestic maritime transport emissions by 2030 relative to the 2005 level. Among key measures are CO_2 emission standards for maritime transports under the jurisdiction of the public sector. As a prominent example, new high-speed passenger vessel services provided by regional governments are expected to face zero emission requirements by 2025.

There are many barriers for diffusion of zero emission vessels, especially in the short run. While energy carriers such as hydrogen or its derivatives, including ammonia, appear as promising substitutes for conventional marine fuels (McKinlay et al., 2021), they are still in their infancies. Current uptake mostly concerns marine batteries (Sundvor et al., 2021) and battery electric high-speed passenger vessels will be essential for meeting the Norwegian government's zero emission requirements, especially in the early stages of this energy transition. However, battery technology has drawbacks due to range, but this limitation can, at least to some extent, be alleviated by better planning (Havre et al., 2022).

With this in mind, this paper studies the Zero-Emission passenger Vessel Service Network Design Problem (ZEVSNDP), which deals with how to optimally introduce battery electric vessels for a given passenger vessel service. The ZEVSNDP studied in this paper is a very complex optimization problem, which includes a number of decisions/features, summarized as follows: (1) determination of vessel routes, where we also allow for complex non-cyclic route structures, e.g., butterfly routes; (2) determination of service frequencies (which can vary for different sub-routes, e.g., in a butterfly route); (3) determination of sailing speeds along the routes; (4) frequency-dependent demand; (5) considering

* Corresponding author.
E-mail address: kjetil.fagerholt@ntnu.no (K. Fagerholt).

https://doi.org/10.1016/j.ejor.2023.11.015
Received 17 April 2023; Accepted 10 November 2023
Available online 14 November 2023

both operator and passenger (transit and waiting time) costs; (6) considering multiple time periods with different demand patterns, which again allows for having different routes, frequencies, and sailing speeds among the time periods; (7) determination of the number and type of vessel to use on the given service; and finally (8) determination of charging infrastructure location(s).

Several papers discuss the transition to zero emission vessels (e.g., Grzelakowski et al., 2022; McKinlay et al., 2021; Reusser & Osses, 2021). However, their emphasis is largely on technical feasibilities and measures to curb greenhouse gas emissions. This is also in line with the emphasis of decision makers in charge of reforming the transport sector in Norway. However, *better planning* of maritime operations through the use of Operations Research (OR) can be essential both to reduce the costs of and enable zero emission transport. Kontovas (2014) conceptualizes the green ship routing and scheduling problem by outlining ways in which ship emissions can be incorporated into OR on maritime transports. In a recent paper, Ritari et al. (2021) study routing and speed optimization of hybrid ships. Unlike this strand of research, the current paper's emphasis is not on minimizing or limiting air emissions from diesel or hybrid vessel operations, but to accommodate zero emission vessel operations in a cost-effective manner.

Havre et al. (2022) introduced the Zero-Emission Vessel Route Planning Problem (ZEVRPP), which to our knowledge is the first decision support model for a zero emission passenger vessel service. Their planning problem seeks to jointly minimize operator and passenger costs *for a given cyclic route* subject to strategic (fleet selection and land-based infrastructure location), tactical (frequency), and operational (sailing speeds) decisions. The ZEVSNDP studied in this paper extends the contribution of Havre et al. (2022) by accommodating multiple planning periods (with different demand patterns) and by considering *route decisions* as a key measure for ensuring technical feasibility and reducing abatement costs (i.e., the costs of removing CO_2 emissions) of battery electric high-speed vessels.

While there are several other studies on optimization of passenger vessel services – including Lai and Lo (2004), Aslaksen et al. (2020, 2021) – preceding (Havre et al., 2022), none pay attention to constraints related to operation of zero emission vessels. Examples include energy storage and charging time constraints. These comparable studies also assume demand to be predetermined and not dependent on service frequency. Following Klier and Haase (2015), we assume on the contrary for the ZEVSNDP that the level of service (frequency) affects the demand for the vessel service.

Most comparable studies on planning problems for zero emission transport – including Rinaldi et al. (2018), Sassi and Oulamara (2017), Zhang et al. (2021), Rogge et al. (2018), and Villa et al. (2020) – are not as rich in characterizing the dynamics of zero emission transport as the ZEVSNDP, as they do not jointly optimize energy use, storage, and infrastructure location. For example, drawing on Andersson et al. (2015), Fagerholt et al. (2010), and Ritari et al. (2021), the ZEVSNDP models the interactions among speed choice and energy use. The combination of frequency (affecting demand) and sailing speed optimization is a novel contribution to the literature on public transport problems.

The ZEVSNDP is a planning problem within public transport. Buba and Lee (2019) consider the Urban Transit Network Design Problem for a homogeneous fleet of buses that, similar to the ZEVSNDP, simultaneously optimizes routes and service frequencies. Their approach involves constructing feasible routes on urban roads with predefined stops, which is parallel to the approach used for the ZEVSNDP. Both problems encompass passengers' and operator's perspectives. This perspective is also adopted by Liu et al. (2022), who study routing of electric buses. Liu et al. (2022) formulate the Urban Electric Transit Network Problem that simultaneously decides bus route layout, service frequency and location and size of electrical charging stations. Arbex and da Cunha (2015) propose a heuristic for a multi-objective Transit Network Design and Frequency Setting Problem to determine an optimal set of routes and the number of times each route is served. However, none of these consider speed optimization, which is more relevant in the maritime setting.

In the maritime setting, Aslaksen et al. (2020) present a Ferry Service Network Design Problem. To solve the problem, the authors propose a two-step approach, where they first generate routes and corresponding frequencies using a construction heuristic. The model then determines the optimal combination of routes, frequencies and vessels that maximizes customer satisfaction. Aslaksen et al. (2020) denote the combination of routes, frequencies and vessels a *rotation*, an approach which is adopted for the ZEVSNDP alongside several other studies. Brouer et al. (2014) study the Liner Shipping Network Design Problem (LSNDP), which also has some similarities with the ZEVSNDP, though for cargo (container) vessels. Their model is designed for handling butterfly rotations, which complicates the assignment of transshipment costs. Brouer et al. (2014) define a *rotation* as a specific configuration of such a service, with a specific vessel class, number of vessels and their sailing speed. Thun et al. (2017) propose a branch-and-price algorithm for solving the LSNDP for different route instances. Similar to what we do in this paper, they consider different route layouts, e.g., butterfly routes. They define a rotation as a given sequence of ports to visit, the vessel type serving these ports and the number of vessels used. In contrast to the ZEVSNDP, the LSNDP usually considers demand and service frequencies as given. Furthermore, the LSNDP does neither include multiple time periods (with different demand patterns) nor considerations about charging and its infrastructure.

To summarize this literature review, the ZEVSNDP is positioned in the literature on public transport problems but it encompasses, as pointed out above, several sub-problems that have been sparsely studied in public transport planning. The problem that is most similar to the ZEVSNDP is the one studied by Havre et al. (2022). However, as described above ZEVSNDP further extends the contributions by Havre et al. (2022) in several ways where the most notable extensions are as follows: (a) while (Havre et al., 2022) consider the route as given, the routes are a decision in the ZEVSNDP, (b) our model allows the modeling of supplementary and more advanced route structures (e.g., butterfly routes) compared to Havre et al. (2022), who only can handle simple cyclical routes (given as input), and (c) we consider multiple time periods with different demand patterns.

Hence, the main contributions of this paper are as follows: First, we define the ZEVSNDP, which extends the work by Havre et al. (2022) in the ways described above, and formulate a novel Mixed Integer Programming (MIP) model for the problem. Second, we test our model and provide several interesting insights on the introduction of zero emission high-speed passenger vessel services for a real case study in Florø, Norway, catering both remote islands and mainland ports that offer substitute transportation. We experience changes to existing routes as being politically sensitive. However, well-informed environmental policies call for comprehensive mapping of their costs and benefits, which is among the current paper's main aims. Thereby, pros and cons can clearly be communicated to decision makers and constituencies alike to promote better policy making and acceptability of environmental legislation. Finally, since the MIP model is too complex to be solved to optimality for real problems, we propose, as a secondary objective, a Decomposition-Based (DB) heuristic for solving the ZEVSNDP.

This paper is structured as follows. Section 2 formally defines the ZEVSNDP, while in Section 3, we propose the MIP model for the ZEVSNDP. Section 4 presents the DB heuristic. Section 5 presents our case study, before we present the computational analyses in Section 6. Finally, we conclude in Section 7.

2. Problem definition

This section formally defines the ZEVSNDP. We consider a set of ports visited throughout a regular service day. The day is divided

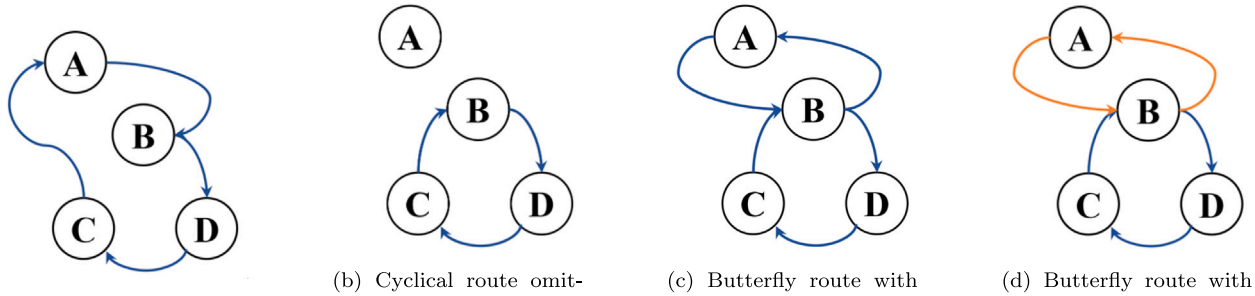

(a) Simple cyclical route (b) Cyclical route omitting one port (c) Butterfly route with two wings (d) Butterfly route with two subroutes

Fig. 1. Example showing some of the different type of routes that can be chosen.

in (equally long) periods with predefined demand for transportation between port pairs for each period. Further, distances between ports are known, enabling the calculation of sailing times for different speed levels.

A route from a set of predefined candidate routes must be chosen in each period to serve the demand. Each candidate route defines a sequence of ports, enabling diverse route structures as exemplified in Fig. 1, e.g., *simple cycles* (Fig. 1(a)), *butterfly* (Fig. 1(c)) and *chain routes*. Simple cycle routes only allow for one stop in each port per round trip, whereas butterfly routes have a central hub, where multiple stops are allowed. The chain route (Thun et al., 2017) is an extension of the butterfly route. This route structure allows for multiple central hubs in one route. It is suitable for routes along a coastline or in a fjord by allowing port stops in both directions. Note that we allow omitting ports in the chosen route, as illustrated in Fig. 1(b), if that is found beneficial.

An essential part of the routes included in the set of candidate routes is its (optional) division into *subroutes*. This allows a route to be operated by separate smaller routes, each having its own number of vessels in use and service frequency. The division into subroutes is highly relevant for routes with a butterfly structure, where the same or separate vessels may serve the different wings of a route, utilizing the central port as a transit hub. Figs. 1(c) and 1(d) show a butterfly route with two wings, and with port B as a hub. In the first case, both wings are served by the same vessel (illustrated with similar colors on the two wings), while in the second case, the different colors indicate that the wings are served by different vessels. In the latter case (Fig. 1(d)), we refer to the two wings as subroutes since they are operated by different vessels and can have different frequencies.

Each route and subroute has a set of potential service frequencies to choose among. Although the demand for transportation is given, we assume that the demand for using the passenger vessel service is dependent on the chosen frequency, e.g., with a reduced service frequency, passengers may choose other modes of transportation. Passengers choosing other means of transportation are considered *unmet demand* in the ZEVSNDP, which has a given cost. Moreover, unmet demand can also stem from two other phenomena. The first is simply from insufficient capacity of the vessels servicing the route. Since we allow choosing routes which omit servicing some ports, we might also have unmet demand between ports not being included in the chosen route.

A number of battery electric vessels from a set of candidate vessel types must be chosen to serve the routes. Each vessel is associated with an investment cost, a crew cost, a passenger capacity, speed range and a speed-dependent energy consumption profile. Each vessel has a given battery size and energy storage capacity, restricting the vessel's range. We only allow for one vessel type to be chosen to ensure a realistic route plan where all departures are treated equally within a port pair, due to being served by similar vessels at all times. Onshore infrastructure must be installed in one or several ports along the route to charge the vessels' batteries. An estimate of the investment cost and the rate of energy transfer (i.e., charging speed), depending on the grid capacity, are assumed known for each potential port where charging infrastructure can be installed.

We consider the passengers to have a *value of time*. The value of time allows to convert both the waiting and sailing time experienced by the passenger to a monetary value. The precise level of the passengers' value of time depends on multiple factors, as discussed by Wardman (2001). We assume two different values of time, one for the time waiting in port and one for the time spent sailing. The conversion between time and monetary units for the passengers enable a single objective problem.

The ZEVSNDP considers decisions at the strategic, tactical and operational planning levels. The strategic decisions are the vessel type and number of vessels to acquire, in addition to at which port(s) to install charging infrastructure. The tactical decisions are which route (including sub-routes) to select, and for each subroute determine how many vessels to use and with which frequency to sail. The operational decisions consist of determining the passenger flow (how many passengers to transport between each port pair), the speed on each sailing leg of the chosen route, and the time spent on various operations for the time period under consideration, i.e., how much time to spend sailing, charging and waiting at the different ports. The time spent charging and the sailing speeds on the legs also give the battery level when leaving each port. The passenger flow is restricted by the passenger capacity of the chosen vessels. Similarly, the energy usage cannot exceed the vessels' battery capacities. Lastly, the service schedule is restricted by the length of the planning periods.

The tactical and operational decisions are made for each time period of the day, while the strategic investment decisions are made for all periods simultaneously. The objective of the ZEVSNDP is to minimize the total system cost, defined as the sum of operator and passenger costs. The operator costs consist of the sum of the vessel investment costs, the crew cost, the infrastructure investment costs, and the energy cost of the vessel service. The passenger costs are defined as the sum of the passengers' cost of alternative transportation (unmet demand), the cost of waiting in port, and the passengers' sailing time costs.

The main focus of the problem is to consider the strategic decisions and provide managerial support for these decisions. However, the tactical and operational decisions are included as they affect the strategic ones.

3. Mathematical formulation

In this section we present a MIP model of the ZEVSNDP in Section 3.3. However, we begin by describing the modeling approach and assumptions in Section 3.1, and the notation used in Section 3.2. In the end of the section, in Section 3.4, we briefly discuss how the proposed model is linearized and solved.

3.1. Modeling approach and assumptions

It is assumed that every port has the possibility to install charging infrastructure, but at different costs based on the state of the available electrical grid at the port. Furthermore, it is assumed that charging of vessels happens at constant power, meaning there is a linear relationship between time spent charging and the battery level. This is considered a fair assumption since we only allow the batteries' state of charge to be within restricted minimum and maximum levels to preserve the batteries' lifetime, e.g., between 40% and 80%.

The modeling of demand is an important aspect of the ZEVSNDP. In general, the demands among all port pairs for all time periods are assumed known. For the ZEVSNDP to handle the demand data, it must be altered to account for ports being in different subroutes and when in the subroutes these are visited. To do so we introduce a demand parameter for each subroute c (in route r in time period p), D_{prckl}, describing the demand from the port at the beginning of leg k to the port at the beginning of leg l within a subroute. Further, the model should comply with passengers wanting to travel from one subroute to another. This is accomplished by routing the passengers through the nearest port linking the two subroutes, e.g., the central hub of a butterfly route.

For each subroute, we can choose among a set of predefined candidate service frequencies. The chosen frequency also affects the passengers' waiting time in port. In the formulation of the ZEVSNDP, a similar approach as that of Shang et al. (2019) is used, where the average waiting time for the passengers is calculated in advance for each possible frequency.

Passengers preferring other means of transportation are considered unmet demand in the model. This could occur, as described in Section 2, when the passenger finds the service frequency insufficient, but it could also occur if the chosen vessels have inadequate capacity to bring all passengers. A third possibility leading to unmet demand, is when the port of origin or destination is omitted in the chosen route. Hence, the cost of passengers using other means of transportation due to a port not being visited is calculated in advance for each potential route choice in each period.

The modeling of time and sailing speed is important in the ZEVSNDP, especially since there is a non-linear relationship between sailing speed and energy consumption. The sailing time along each leg is computed in advance for a discrete number of speeds. A vessel can then be assigned a speed which is a linear combination of the discrete speed levels, following the approach proposed by Andersson et al. (2015).

3.2. Notation

Let each time period within the planning horizon be represented by an index $p \in \mathcal{P}$, and let each period be of length $\overline{T}_p$. In each period p, a single route may be chosen from a set of potential candidate routes, $\mathcal{R}_p$. Further, a route r consists of a set of subroutes C_r. A subroute c contains a set of legs, $\mathcal{K}_c$ and ports, $\mathcal{I}_c$, where the set of ports in a subroute is a subset of all ports, $\mathcal{I}$. Let $\mathcal{F}_c$ be the set of potential service frequencies in each subroute. The set of available candidate vessel types is given by $\mathcal{V}$. Each potential vessel type, v, has a set of discrete speed levels, S_v, which can be linearly combined to achieve continuous speed selection, as described in Section 3.1.

The time of sailing a leg k, in a subroute c (in a route r in time period p), with a vessel v, at speed s, is computed in advance and denoted T_{prckvs}. Further, a vessel has a minimum waiting time in each port $\underline{T}_i^W$, representing time spent on docking and embarking/disembarking passengers. The travel time from the port at the beginning of leg k, to the port at the beginning of leg l, in subroute c (in a route r in time period p), sailed with the fastest available vessel type at its highest speed level, is given by the parameter T^U_{prckl}. The parameter W_{prcf} represents the passenger waiting time in a port, dependent on the frequency f in subroute c (in a route r in time period p) as discussed in Section 3.1.

Let D_{prckl} denote the maximum demand for transportation from the port at the beginning of leg k, to the port at the beginning of leg l, within subroute c (in a route r in time period p). As explained in Section 2, lower frequencies lead to passengers preferring other means of transportation, while higher frequencies make the service more attractive. Thus, the parameter D^F_{prcklf} is introduced to represent the frequency-dependent demand for passengers with origin port at the beginning of leg k, with destination port at the beginning of leg l, in subroute c, when served with frequency f, in time period p. Note that the maximum demand for transportation, D_{prckl}, is equal to the demand for transportation at the highest available service frequency, $|\mathcal{F}_c|$, implying that $D_{prckl} = D^F_{prckl|\mathcal{F}_c|}$. Lastly, the served demand is restricted by the capacity of the chosen vessel type, v, denoted Q_v.

A vessel must at all times demonstrate a battery level above a lower bound, $\underline{B}_v$, and below a maximum bound, $\overline{B}_v$. The energy consumption when sailing a leg k, in subroute c (in a route r in time period p), with vessel type v, at speed level s, is denoted E_{prckvs}. Further, each subroute must contain a port with charging infrastructure installed, to ensure feasibility of the route. Since the location of infrastructure is a strategic decision that cannot be changed across time periods, we need to know the port i where leg k starts in each subroute c, in a route r in time period p. To do so, we introduce the parameter A_{prcik}, which is equal to 1 if leg k starts at port i in subroute c, and 0 otherwise. Lastly, P_i denotes the potential charging power that could be installed in port i.

As explained in Section 2, the ZEVSNDP considers both the operator and passenger costs. The first of the operator's costs is the vessel investment cost for each vessel type C^{FC}_v. Further, there is an investment cost, C^{INF}_i, for installing infrastructure in port i. We let C^{VC}_{pi} denote the energy cost per kWh in period p in port i. The last operator cost is denoted C^{CREW}_v, representing the crew cost associated with using a vessel of type v for one hour. When considering the passenger costs, there is a cost incurred by passengers choosing other means of transportation. Let the parameter C^{ALT2}_{prckl} denote the cost of one such passenger demanding transportation from the port starting at leg k, to the port starting at leg l, in subroute c (in a route r in time period p). The cost of unmet demand due to omitting any origin or destination ports along route r in time period p is computed directly and labeled C^{ALT1}_{pr}. Lastly, we denote C^{PW} and C^{SW} as the value of passenger time while waiting in port and the value of passenger time while sailing, respectively.

We also use a number of big-M parameters in the model, i.e., M^1 – M^7 (with different indices). The value of each of these is calculated to be as small as possible, but still sufficiently large.

The strategic decisions are given by the following variables: Let α_i be a binary variable, equal to 1 if infrastructure is installed at port i, and 0 otherwise. Let δ_v be a binary variable, equal to 1 if vessel type v is chosen, and 0 otherwise. Let y_v be an integer variable, denoting the number of vessels of type v acquired.

The tactical decisions are given by the following variables: Let β_{pr} be a binary variable, equal to 1 if route r is chosen in time period p, and 0 otherwise. Let g_{prcv} be an integer variable, denoting the number of vessels of type v used in subroute c in route r in period p. Let z_{prcf} be a binary variable, equal to 1 if frequency f is chosen for subroute c in route r in time period p, and 0 otherwise.

The operational decisions are given by the following variables: Let $x_{prckvfs}$ denote the weight variable for the speed level s for a vessel of type v on leg k when subroute c is served with frequency f, in a route r in time period p. This allows for a linear combination of the speed levels. Let $c_{prcikvf}$ and $w_{prcikvf}$ denote the charging and waiting times in port i before sailing leg k with a vessel of type v in subroute c served with frequency f (in a route r in time period p), respectively. Let t^{RT}_{prcvf} denote the round trip time for a vessel of type v in subroute c sailing with frequency f in route r in period p. Let t_{prckl} be the transit time from the port at the beginning of leg k, to the port at the beginning of

leg l, in subroute c, in route r, in time period p. Lastly, let b_{prckv} denote the battery level before sailing leg k, with a vessel of type v, in subroute c, in route r, in time period p. Let $q_{prcklvf}$ be the number of passengers picked up in the port at the beginning of leg k, with destination port at the beginning of leg l, in subroute c, in route r, in time period p, served with frequency f, and vessel type v. Let l_{prcklv} denote the number of passengers on board a vessel of type v, on leg k, with destination port at the beginning of leg l, in subroute c in route r, in time period p. Let u_{prckl} denote the number of passengers using other means of transportation from the port at the beginning of leg k, with destination port at the beginning of leg l, in subroute c, when route r is chosen in time period p. These variables only consider the passengers that use other means of transportation, but potentially could use the vessel service. The unmet demand due to either the origin or destination port not being visited in the route, is already incorporated in the parameter C^{ALT1}_{pr}, as described above.

A summary of the notation is presented in Appendix A.

3.3. Zero emission vessel model

In the following we present the mathematical formulation of the *zero emission vessel model*. It should be noted that we present the model including some non-linear terms (which are later linearized), both in the objective function and some of the constraints, as this presentation is more intuitive and easier to understand.

Objective function

We define the following objective function.

$$\begin{aligned}\min z = &\sum_{v\in\mathcal{V}} C^{FC}_{v} y_v + \sum_{i\in\mathcal{I}} C^{INF}_{i}\alpha_i \\ &+ \sum_{p\in\mathcal{P}}\sum_{r\in\mathcal{R}_p}\sum_{c\in\mathcal{C}_r}\sum_{i\in\mathcal{I}_r}\sum_{k\in\mathcal{K}_c}\sum_{v\in\mathcal{V}}\sum_{f\in\mathcal{F}_c} C^{VC}_{pi} P_i c_{prcikvf} z_{prcf} \\ &+ \sum_{p\in\mathcal{P}}\sum_{r\in\mathcal{R}_p}\sum_{c\in\mathcal{C}_r}\sum_{v\in\mathcal{V}} C^{CREW}_{v}\overline{T}_p g_{prcv} + \sum_{p\in\mathcal{P}}\sum_{r\in\mathcal{R}_p} C^{ALT1}_{pr}\beta_{pr} \\ &+ \sum_{p\in\mathcal{P}}\sum_{r\in\mathcal{R}_p}\sum_{c\in\mathcal{C}_r}\sum_{k\in\mathcal{K}_c}\sum_{l\in\mathcal{K}_c} C^{ALT2}_{prckl} u_{prckl} \\ &+ C^{PW}\sum_{p\in\mathcal{P}}\sum_{r\in\mathcal{R}_p}\sum_{c\in\mathcal{C}_r}\sum_{f\in\mathcal{F}_c} W_{prcf} z_{prcf}\Big(\sum_{k\in\mathcal{K}_c}\sum_{l\in\mathcal{K}_c} q_{prcklvf}\Big) \\ &+ C^{SW}\sum_{p\in\mathcal{P}}\sum_{r\in\mathcal{R}_p}\sum_{c\in\mathcal{C}_r}\sum_{k\in\mathcal{K}_c}\sum_{l\in\mathcal{K}_c}\sum_{f\in\mathcal{F}_c}(t_{prckl} - T^{U}_{prckl}) D_{prcklf} z_{prcf}\end{aligned} \tag{1}$$

The objective function (1) aims to minimize the total system costs. The first four terms cover the operator costs, while the last four terms encompass the passenger costs. The first two terms represent the investments costs of vessels and infrastructure, respectively. The third term is the variable cost of charging. The last operator cost, given in fourth term, is the crew cost. The fifth and sixth terms represent the alternative cost of using other means of transportation. The former captures the alternative cost of not visiting a port in the chosen route r in period p. The sixth term calculates the cost of passengers using other means of transportation, when both origin and destination port is served by the chosen route. The seventh term computes the passengers' cost of waiting in port, which depends on the frequency. The last term in the objective function encompasses the passengers' costs of transit time, where the difference between actual transit time, t_{prckl}, and the minimum sailing time (obtained with the highest sailing speed), T^{U}_{prckl}, is penalized.

Constraints linking strategic and tactical decisions

Constraint (2) makes sure we only choose vessels of one type. Next, Constraints (3) allow the model to only invest in vessels of the chosen vessel type v. Constraints (4) ensure that exactly one route is chosen in each time period. Constraints (5) make sure only one frequency is chosen for each subroute c in the chosen route r. Constraints (6) restrain the number of vessels used in each time period to being less than or equal to the number of vessels acquired. Constraints (7) ensure the frequency in a subroute c to be greater than or equal to the number of vessels used in the subroute, to prevent vessels only sailing a partial round trip.

$$\sum_{v\in\mathcal{V}} \delta_v = 1 \tag{2}$$

$$y_v \le M^1 \delta_v, \qquad v\in\mathcal{V} \tag{3}$$

$$\sum_{r\in\mathcal{R}_p} \beta_{pr} = 1, \qquad p\in\mathcal{P} \tag{4}$$

$$\sum_{f\in\mathcal{F}} z_{prcf} = \beta_{pr}, \qquad p\in\mathcal{P},\ r\in\mathcal{R}_p,\ c\in\mathcal{C}_r \tag{5}$$

$$\sum_{r\in\mathcal{R}_c}\sum_{c\in\mathcal{C}_r} g_{prcv} \le y_v, \qquad p\in\mathcal{P},\ v\in\mathcal{V} \tag{6}$$

$$\sum_{v\in\mathcal{V}} g_{prcv} \le \sum_{f\in\mathcal{F}} f z_{prcf}, \qquad p\in\mathcal{P},\ r\in\mathcal{R}_p,\ c\in\mathcal{C}_r \tag{7}$$

Time constraints

The following constraints handle the relationship between round trip time, sailing speed and frequency. Constraints (8) define the round trip time as the sum of the sailing time, waiting time and charging time along the subroute. Constraints (9) make sure the frequency multiplied by the round trip time along a subroute c equals the length of the planning period in the period multiplied by the number of vessels used in the subroute. The waiting time in each port must be greater than the minimum waiting time, T^{w}_{i}, ensured by Constraints (10). Note the use of the binary parameter A_{prcik}, which associates the leg k with the port at its origin i. For vessel types that are not chosen we set the waiting time to zero through Constraints (11), while for frequencies and routes not chosen this is assured by Constraints (12). Constraints (13) make sure the speed weight variable sums up to one, for each leg k, in each subroute c, for the chosen route r and frequency f, and the chosen vessel type v for each time period p. Lastly, Constraints (14) and (15) define the transit time between the port at the beginning of leg k to the port at the beginning of leg l, in subroute c, in route r, in time period p. It should be noted that the charging and waiting time at the port at the beginning of leg k and leg l is excluded from the transit time between the ports, since it will not affect the passengers' transit time on board.

$$t^{RT}_{prcvf} = \sum_{k\in\mathcal{K}_c}\sum_{s\in\mathcal{S}_v} T_{prckvs} x_{prckvfs} + \sum_{k\in\mathcal{K}_c}\sum_{i\in\mathcal{I}_c}(c_{prcikvf} + w_{prcikvf}), \qquad p\in\mathcal{P},\ r\in\mathcal{R}_p,\ c\in\mathcal{C}_r,\ v\in\mathcal{V},\ f\in\mathcal{F}_c \tag{8}$$

$$\sum_{f\in\mathcal{F}_c}\sum_{v\in\mathcal{V}} f z_{prcf} t^{RT}_{prcvf} = \overline{T}_p \sum_{v\in\mathcal{V}} g_{prcv}, \qquad p\in\mathcal{P},\ r\in\mathcal{R}_p,\ c\in\mathcal{C}_r \tag{9}$$

$$w_{prcikvf} \ge \underline{T}^{w}_{i} A_{prcik} z_{prcf}\delta_v, \qquad p\in\mathcal{P},\ r\in\mathcal{R}_p,\ c\in\mathcal{C}_r\ v\in\mathcal{V},\ i\in\mathcal{I}_c,\ k\in\mathcal{K}_c,\ f\in\mathcal{F}_c \tag{10}$$

$$w_{prcikvf} \le M^2_{prc} A_{prcik}\delta_v, \qquad p\in\mathcal{P},\ r\in\mathcal{R}_p,\ c\in\mathcal{C}_r,\ i\in\mathcal{I}_c,\ k\in\mathcal{K}_c,\ v\in\mathcal{V},\ f\in\mathcal{F}_c \tag{11}$$

$$w_{prcikvf} \le M^3_{prc} A_{prcik} z_{prcf}, \qquad p\in\mathcal{P},\ r\in\mathcal{R}_p,\ c\in\mathcal{C}_r,\ i\in\mathcal{I}_c,\ k\in\mathcal{K}_c,\ v\in\mathcal{V},\ f\in\mathcal{F}_c \tag{12}$$

$$\sum_{s\in\mathcal{S}_v} x_{prckvfs} = \delta_v z_{prcf}, \qquad p\in\mathcal{P}, r\in\mathcal{R}_p, c\in\mathcal{C}_r,\ k\in\mathcal{K}_c,\ v\in\mathcal{V},\ f\in\mathcal{F}_c \tag{13}$$

$$t_{prckl} = \sum_{v\in\mathcal{V}}\sum_{f\in\mathcal{F}_c}\left[\sum_{\hat{k}=k}^{l-1}\sum_{s\in S_v} T_{prc\hat{k}vs}x_{prc\hat{k}vfs} + \sum_{i\in\mathcal{I}_c}\sum_{\hat{k}=k+1}^{l-1}(c_{prci\hat{k}vf} + w_{prci\hat{k}vf})\right], \quad p\in\mathcal{P},\ r\in\mathcal{R}_p,\ c\in\mathcal{C}_r,\ k\in\mathcal{K}_c,\ l\in\mathcal{K}_c \mid l>k \tag{14}$$

$$t_{prckl} = \sum_{v\in\mathcal{V}}\sum_{f\in\mathcal{F}_c}\left[\sum_{\hat{k}=k}^{|\mathcal{K}_c|}\sum_{s\in S_v} T_{prc\hat{k}vs}x_{prc\hat{k}vfs} + \sum_{i\in\mathcal{I}_c}\sum_{\hat{k}}^{|\mathcal{K}_c|}(c_{prci\tilde{k}vf} + w_{prci\tilde{k}vf}) + \sum_{k'}^{l-1}\left(\sum_{s\in S_v} T_{prck'vs}x_{prck'vfs} + \sum_{i\in\mathcal{I}_c}(c_{prcik'vf} + w_{prcik'vf})\right)\right], \quad p\in\mathcal{P},\ r\in\mathcal{R}_p,\ c\in\mathcal{C}_r,\ k\in\mathcal{K}_c,\ l\in\mathcal{K}_c \mid k>l \tag{15}$$

where,

$\tilde{k} = \min\{|\mathcal{K}_c|, k+1\}$

$k' = \max\{1, l-1\}$

Battery constraints

Constraints (16) and (17) keep track of the battery level along the route. It should be noted that Constraints (17) are included to capture the relationship between the last leg in the set of ports and the first, thus ensuring we finish with the same battery level as we started with. Furthermore, Constraints (18) and (19) make sure the battery level does not exceed its maximum and minimum limits, respectively. Constraints (20) ensure that charging is only possible at the ports where charging infrastructure is installed. Lastly, Constraints (21) and (22) ensure that the charging time variable cannot take values for routes, frequencies and vessel types not chosen.

$$b_{prckv} = b_{prc,k-1,v} - \sum_{f\in\mathcal{F}_c}\sum_{s\in S_v} E_{prc,k-1,vs}x_{prc,k-1,vfs} + \sum_{i\in\mathcal{I}_r}\sum_{f\in\mathcal{F}_c} A_{prcik}P_i c_{prcikvf}, \quad p\in\mathcal{P},\ r\in\mathcal{R}_p,\ c\in\mathcal{C}_r,\ k\in\mathcal{K}_c\backslash\{1\},\ v\in\mathcal{V} \tag{16}$$

$$b_{prc1v} = b_{prc,|\mathcal{K}_c|,v} - \sum_{f\in\mathcal{F}_c}\sum_{s\in S_v} E_{prc,|\mathcal{K}_c|,vs}x_{prc,|\mathcal{K}_c|,vfs} + \sum_{i\in\mathcal{I}_c}\sum_{f\in\mathcal{F}_c} A_{prcik}P_i c_{prci,1,vf}, \quad p\in\mathcal{P},\ r\in\mathcal{R}_p,\ c\in\mathcal{C}_r\ v\in\mathcal{V} \tag{17}$$

$$b_{prckv} \le \overline{B}_v\delta_v\beta_{pr}, \quad p\in\mathcal{P},\ r\in\mathcal{R}_p,\ c\in\mathcal{C}_r,\ k\in\mathcal{K}_c,\ v\in\mathcal{V} \tag{18}$$

$$b_{prckv} - \sum_{f\in\mathcal{F}_c}\sum_{s\in S_v} E_{prckvs}x_{prckvfs} \ge \underline{B}_v\delta_v\beta_{pr}, \quad p\in\mathcal{P},\ r\in\mathcal{R}_p,\ c\in\mathcal{C}_r,\ k\in\mathcal{K}_c,\ v\in\mathcal{V} \tag{19}$$

$$c_{prcikvf} \le M^4_{iv}A_{prcik}\alpha_i,\ p\in\mathcal{P},\ r\in\mathcal{R}_p, c\in\mathcal{C}_r,\ i\in\mathcal{I}_c,\ k\in\mathcal{K}_c,\ v\in\mathcal{V},\ f\in\mathcal{F}_c \tag{20}$$

$$c_{prcikvf} \le M^5_{iv}z_{prcf}, \quad p\in\mathcal{P},\ r\in\mathcal{R}_p, c\in\mathcal{C}_r,\ i\in\mathcal{I}_c,\ k\in\mathcal{K}_c,\ v\in\mathcal{V},\ f\in\mathcal{F}_c \tag{21}$$

$$c_{prcikvf} \le M^6_{iv}\delta_v, \quad p\in\mathcal{P},\ r\in\mathcal{R}_p, c\in\mathcal{C}_r,\ i\in\mathcal{I}_c,\ k\in\mathcal{K}_c,\ v\in\mathcal{V},\ f\in\mathcal{F}_c \tag{22}$$

Passenger flow constraints

We only allow passengers in a subroute to be picked up (or be on board) if a vessel is chosen for the subroute. This is ensured through Constraints (23). Furthermore, we restrict the load on a leg from exceeding the chosen vessel type's capacity through Constraints (24). Constraints (25) and (26) keep track of the number of passengers on board a vessel. The constraints make sure that the number of passengers entering the vessel in a port with a specific destination is the difference between the previous and current passenger load with the same destination. The passengers that potentially could be picked up, are constrained by the number of passengers that wants to use the vessel service at the specific subroute frequency. This is covered by Constraints (27). The unmet demand caused by passengers choosing other means of transportation, even when they have the possibility of using the vessel service, is determined by Constraints (28). Lastly, we define Constraints (29) and (30) to ensure passengers may only disembark the vessel at their destination.

$$l_{prcklv} \le M^7_{prckl}g_{prcv}, \quad p\in\mathcal{P},\ r\in\mathcal{R}_p,\ c\in\mathcal{C}_r,\ k\in\mathcal{K}_c,\ l\in\mathcal{K}_c,\ v\in\mathcal{V} \tag{23}$$

$$\sum_{l\in\mathcal{K}_c} l_{prcklv} \le Q_v\sum_{f\in\mathcal{F}_c} f\, z_{prcf}, \quad p\in\mathcal{P},\ r\in\mathcal{R}_p,\ c\in\mathcal{C}_r,\ k\in\mathcal{K}_c,\ v\in\mathcal{V} \tag{24}$$

$$\sum_{f\in\mathcal{F}_c} q_{prcklvf} = l_{prcklv} - l_{prc,k-1,lv}, \quad p\in\mathcal{P},\ r\in\mathcal{R}_p,\ c\in\mathcal{C}_r, \quad k\in\mathcal{K}_c\backslash\{1\},\ l\in\mathcal{K}_c \mid l\ne k,\ v\in\mathcal{V} \tag{25}$$

$$\sum_{f\in\mathcal{F}_c} q_{prc,1,lvf} = l_{prc,1,lv} - l_{prc|\mathcal{K}_c|,lv}, \quad p\in\mathcal{P},\ r\in\mathcal{R}_p,\ c\in\mathcal{C}_r,\ l\in\mathcal{K}_c\backslash\{1\},\ v\in\mathcal{V} \tag{26}$$

$$q_{prcklvf} \le D^F_{prcklf}\, z_{prcf}, \quad p\in\mathcal{P},\ r\in\mathcal{R}_p,\ c\in\mathcal{C}_r,\ k\in\mathcal{K}_c,\ l\in\mathcal{K}_c,\ f\in\mathcal{F}_c \tag{27}$$

$$\sum_{v\in\mathcal{V}}\sum_{f\in\mathcal{F}_c} q_{prcklvf} + u_{prckl} = D_{prckl}\beta_{pr}, \quad p\in\mathcal{P},\ r\in\mathcal{R}_p,\ c\in\mathcal{C}_r,\ k\in\mathcal{K}_c,\ l\in\mathcal{K}_c \tag{28}$$

$$l_{prc,k-1,l} \le l_{prcklv}, \quad p\in\mathcal{P},\ r\in\mathcal{R}_p,\ c\in\mathcal{C}_r,\ k\in\mathcal{K}_c\backslash\{1\},\ l\in\mathcal{K}_c \mid l\ne k,\ v\in\mathcal{V} \tag{29}$$

$$l_{prc,|\mathcal{K}_c|,lv} \le l_{prc,1,lv}, \quad p\in\mathcal{P},\ r\in\mathcal{R}_p,\ c\in\mathcal{C}_r,\ l\in\mathcal{K}_c\backslash\{1\},\ v\in\mathcal{V} \tag{30}$$

Non-negativity, binary, and integer requirements

The variables are defined as (non-negative) continuous, binary, and integer variables as explained in Section 3.2.

3.4. Model linearization, conventional vessel model, and solution method

Constraints (9), as well as the third, seventh and eighth terms of the objective function are non-linear due to continuous variables being

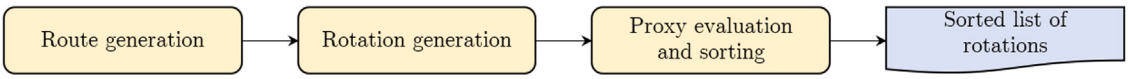

Fig. 2. First step of the DB heuristic.

multiplied with the binary variable, z_{prcf}. Furthermore, in Constraints (10) and (13), the two binary variables δ_v and z_{prcf} are multiplied with each other, in Constraints (18) and (19) the two binary variables δ_v and β_{pr} are multiplied, causing a non-linearity. These non-linear terms are linearized to obtain a linear model, which can then be solved by a commercial MIP-solver (e.g., Gurobi), by using standard linearization techniques in the same way as e.g., in Havre et al. (2022).

The model presented in Section 3.3 has also been adjusted to the use of conventional diesel-fueled vessels. This is relevant for being able to compare solutions with conventional and zero emissions vessels, and to calculate the abatement costs. In doing this, we follow a similar approach as shown in Havre et al. (2022) without going into more details here.

4. Decomposition-based Heuristic solution method

Solving the model in Section 3 to optimality is practically impossible for realistic instances due to the extremely high number of feasible routes, where each route again can be configured into a large number of different subroutes (butterfly wings operated by different vessels), as illustrated in Fig. 1. Hence, we propose a Decomposition-Based heuristic (DB heuristic) to find good solutions to the ZEVSNDP. The main idea of the DB heuristic is to use the peak period (with the highest total demand) to set the strategic decisions, i.e., the infrastructure locations, vessel types and fleet size, and fix the values for these decisions when solving the remaining time periods. The motivation behind this is based on that if a solution is able to serve the period with the highest demand, it will in most practical cases also be able to serve the periods with lower demand in a reasonable way. This also follows the way many planners think when setting up such services in practice. When the strategic decisions are made, the time periods become independent of each other, and we can solve the other time periods separately, thus reducing the solution space and consequently the run time of our model.

The DB heuristic consists of three main steps, where the first step of the solution method is displayed in Fig. 2. The first step is a heuristic route generation. A route is a construct of two pieces of information, a sequence of port visits, the *main route*, and possibly a *subroute* configuration, explaining how the main route is operated in one or more subroutes. The route generation is performed in two separate steps. First, a set of main routes are constructed. These routes are only sequences of ports, and contain no specification of subroute structure. In the second step, we use the main routes as input, and subsequently create routes with all possible configurations of subroutes, for each main route.

Since the number of route combinations grows exponentially with the number of ports, only a subset of all feasible routes can be generated in most practical cases. A good process for generating good and realistic candidate routes is likely to depend on the specific geographical area in consideration. In a practical setting, this could be performed in collaboration with operators, policy makers or other stakeholders, as this step may sometimes touch upon policy-related issues. If a transition from a conventional to a zero emission vessel service is the problem at hand, an example of such a topic could be the allowed degree of change from the original service. In this paper, we have proposed a route generation algorithm where we generate routes with maximum n wings. This algorithm is to some extent tailored for our case study (though it can easily be adapted to other cases and geographical regions) and is described in more detail in Appendix B.

Each route generated is then used to make all possible *rotations*. A rotation is a composition of the essential integer decisions: route (and subroute), frequency, infrastructure, vessels type, number of vessels in total and within each subroute. The rotations are introduced because the fixing of integer variables allows for using the rotations as input to a Linear Program (LP), which is significantly simpler to solve than the full MIP model for the whole ZEVSNDP. When solving the LP for a rotation, the objective value and optimal operational decisions based on the decisions in the rotation are returned.

Before solving the rotations as LPs, we perform an intermediate step. We sort the rotations based on an assessment of their quality, so that only the most promising rotations are solved as LPs. In this process, we introduce a *proxy function* for efficiently evaluating the quality of a rotation by approximating the objective function value of the LP-model for the given rotation. Accordingly, the calculation time is shorter, which allows for sorting the whole set of rotations more efficiently than if the LP-model was solved directly. The sorted list of rotations is now used as input to the second step of the solution method, displayed in Fig. 3.

As shown in Fig. 3, the LP-version of the MIP model successively evaluates the most promising rotations in the sorted list. It is solved exclusively for the peak period, the period with the highest total demand, as it is assumed that this period is most important to consider when making the strategic investment decisions. Several criteria are checked for each rotation. The first criterion is a fast feasibility check, and rotations are discarded if they are infeasible. Conversely, a feasible rotation is stored for later use, and its true objective function value, which can deviate from the approximated one used in the first step of the algorithm, is compared to the current best. If the objective value is better than the current best, we update the best solution found. There are two stop criteria in the method. First, if a sufficient number of feasible solutions, m, are found without updating the current best solution. Second, the method also terminates if it runs for a predefined amount of time, t. After termination, the stored solutions, together with the strategic decisions of the best solution found, are passed to the third and final step of the solution method.

In the final step of the algorithm, a single period MIP model is used to solve each of the remaining time periods to obtain the true objective value for the given strategic decisions. The model is a simplified version of the original MIP model, presented in Section 3, with the only difference being the fixation of strategic decision variables across time periods. These decisions are the infrastructure layout, the vessel type and the total number of vessels. Note that the tactical and operational decisions are allowed to vary among time periods. As the strategic decision variables linking the time periods together are fixed, the single period MIP model allows for solving the time periods independently, which results in a significantly reduced computational effort.

In addition to the strategic decisions, the model is given a set of promising routes from the LP model solutions in step 2. This set is large, and an integral part of obtaining good solutions from the single period MIP model is thus the selection of good, unique and diverse routes from this set. This is accomplished by a route processing that returns a set of r candidate routes. The processing is performed as follows. Every route is split into its respective subroutes. From these routes, new routes that cover all directional combinations of the subroutes are constructed. This accounts for the chance of demand mainly flowing in the opposite direction among different time periods, which would make it beneficial to change the route direction. The resulting set of candidate routes is then used as input for the single period MIP model, which is solved for

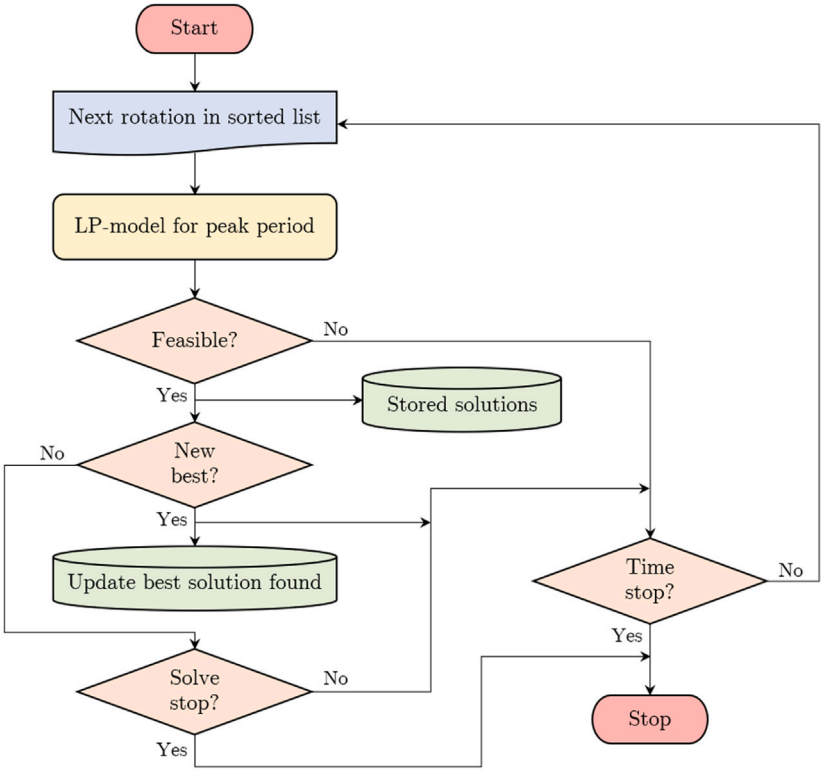

Fig. 3. Second step of the DB heuristic.

the remaining time periods. The solutions from all periods constitute the solution to the full MIP model presented in Section 3.

5. Case study

We consider a case study of an existing high-speed passenger vessel service in Florø, a small coastal city situated on the west coast of Norway. The Florø basin consists of 20 ports, as displayed in Fig. 4. The figure shows the ports divided into three groups ($n = 3$), *North*, *West* and *South*, based on how the area is served today. In the following, we present the relevant data collection in Section 5.1. Further, three test instances based on this data are presented in Section 5.2.

5.1. Input data

Demand data, time periods and frequency levels

The demand data used to create test instances for the ZEVSNDP is based on ticket sales obtained from the operator, Skyss AS. The original dataset contains ticket sales for three months in 2019, i.e., February, March, and April. We have divided the planning horizon (a representative day) into smaller time periods to capture changes in travel pattern over a day. For example, most passengers commute to Florø to work in the morning period, while in the afternoon most of the passenger flow goes in the opposite direction (i.e., from Florø to the surrounding ports). It should be noted that dividing the day into smaller time periods is a trade-off between representing the travel pattern in a good way and how the length of these time periods affect the results. Shorter (and a larger number of) time periods will give a better representation of the true travel pattern (if such detailed and reliable data exists). However, too short time periods will impose limitations on the duration and the length of the routes, which could negatively affect the results. After studying the travel pattern based on the ticket sales, we found that dividing the travel pattern into the following four 4-hour time periods gave a good representation for our model: 5:00 AM - 9:00 AM, 9:00 AM - 1:00 PM, 1:00 PM - 5:00 PM and 5:00 PM - 9:00 PM. Note that there is no operation of the passenger vessel service during night.

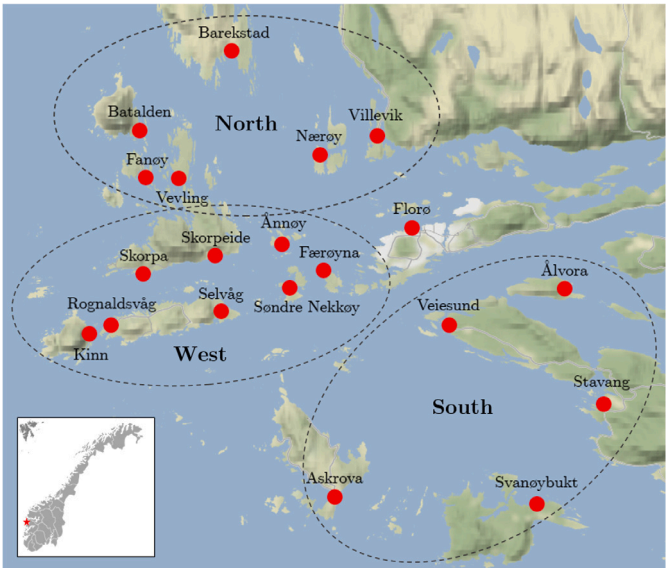

Fig. 4. Map of the ports in the Florø basin, and the current division into port groups.

The candidate service frequencies are $\mathcal{F} = \{1, 2, 3\}$ in each of the four time periods for all test instances presented in Section 5.2. The current frequency, upon which the observed demand data $D_{observed}$ is based, is 1. After consulting with the operator, we use a scaling coefficient of 1.2 resulting in frequency-dependent demand parameters of $(D_{observed})$, $(1.2 \cdot D_{observed})$ and $(1.44 \cdot D_{observed})$ for frequency levels of 1, 2 and 3, respectively. Note that the extrapolation of an observed demand, based on one specific service frequency, to other frequencies,

Table 1
Zero-Emission vessel types (VT) used for the test instances (Havre et al., 2022).

VT	Length (m)	PAX	Cost (mill.)	Battery (kWh)	Speed levels (nm)	Power demand (kW)
1S	30	50	92.9	1000	(10, 15, 20, 25, 30)	(115, 405, 703, 1079, 1637)
1M	30	50	99.8	2000	(10, 15, 20, 25, 30)	(116, 447, 766, 1159, 1737)
1L	30	50	106.7	3000	(10, 15, 20, 25, 30)	(121, 490, 833, 1239, 1841)
2S	30	100	93.9	1000	(10, 15, 20, 25, 30)	(119, 472, 805, 1205, 1798)
2M	30	100	100.8	2000	(10, 15, 20, 25, 30)	(125, 517, 873, 1287, 1904)
2L	30	100	107.7	3000	(10, 15, 20, 25, 30)	(133, 564, 946, 1369, 2013)
3S	30	150	94.9	1000	(10, 15, 20, 25, 30)	(129, 544, 915, 1335, 1967)
3M	30	150	101.8	2000	(10, 15, 20, 25, 30)	(140, 593, 990, 1418, 2078)
3L	30	150	108.7	3000	(10, 15, 20, 25, 30)	(153, 644, 1068, 1503, 2193)
4S	30	200	95.9	1000	(10, 15, 20, 25, 30)	(147, 622, 1035, 1467, 2145)
4M	30	200	102.8	2000	(10, 15, 20, 25, 30)	(162, 674, 1115, 1553, 2261)
4L	30	200	109.7	3000	(10, 15, 20, 25, 30)	(179, 729, 1199, 1640, 2381)
5S	40	200	117.8	2000	(10, 15, 20, 25, 30)	(104, 347, 954, 1416, 2225)
5M	40	200	128.2	3500	(10, 15, 20, 25, 30)	(114, 374, 1019, 1513, 2350)
5L	40	200	138.5	5000	(10, 15, 20, 25, 30)	(124, 404, 1087, 1613, 2477)
6S	40	250	118.8	2000	(10, 15, 20, 25, 30)	(114, 376, 1023, 1518, 2357)
6M	40	250	129.2	3500	(10, 15, 20, 25, 30)	(124, 406, 1091, 1618, 2484)
6L	40	250	139.5	5000	(10, 15, 20, 25, 30)	(135, 438, 1163, 1721, 2614)
7S	40	300	119.8	2000	(10, 15, 20, 25, 30)	(125, 408, 1095, 1624, 2491)
7M	40	300	130.2	3500	(10, 15, 20, 25, 30)	(135, 440, 1167, 1727, 2621)
7L	40	300	140.5	5000	(10, 15, 20, 25, 30)	(147, 474, 1241, 1833, 2752)

may easily be changed. An option could be to incorporate the elasticity of demand based on empirical studies (Totten & Levinson, 2016).

Vessel data

Similar to Havre et al. (2022), we define 21 realistic battery electric vessel types based on data from a maritime consulting agency involved in the project. The vessel types with their features are shown in Table 1. Note the conventions for naming the vessel types. The names of the candidate vessels consist of a number and a letter. The numbers are decided by the length and passenger capacity, where a low number corresponds to small dimensions, whereas a higher number corresponds to larger dimensions. The letters divide the vessels with the same numbers with respect to battery size. Letters S, M and L correspond to Small, Medium and Large batteries, respectively. Note also that the 30-meter vessel types have battery capacities of 1000, 2000 and 3000 kWh, while the 40-meter vessel types have battery capacities of 2000, 3500 and 5000 kWh, as advised by the maritime consulting agency.

A set of conventional diesel vessel types is also defined for the comparison between zero emission and conventional vessels. Here, we assume that the conventional vessels have the same sizes as the zero emission vessels, resulting in seven conventional vessel types (as there is no differentiation by battery capacity). We thus introduce the naming convention nC for conventional vessels, where n refers to the same number as in for Zero Emission, while C means Conventional.

Cost parameters

The model takes several cost parameters as input. The first cost in the objective function is the fixed cost of acquiring a vessel of each type, C_v^{FC}, shown in Table 1. This investment cost is scaled to the length of the planning horizon (i.e., one day), which is done by assuming a standard lifetime of the vessels of 20 years and an interest rate of 5% to calculate the cost of capital per day for the vessel investments. The infrastructure investment cost is estimated to 12 MNOK, similar for all ports, based on data obtained from Statkraft, a Norwegian energy company. The calculation of the daily (capital) cost of the investment in charging infrastructure follows the same procedure as for the vessels. We assume the same yearly rate and usage per day as for the vessels. The third cost parameter, C_{pi}^{VC}, is the energy cost per kWh of charged energy in a port i, in period p. This parameter value is also based on the data obtained from Statkraft, and is set to 3.1 NOK/kWh. The energy cost per outputted kWh is estimated to be 3.0 NOK for the conventional vessel set. Here we assume an MGO (marine gas oil) price of 1100 USD/ton, a conversion rate of 9.74 NOK/USD, an MGO heating value of 42.7 kJ/g and a thermodynamic efficiency of 30%. The heating value and efficiency are inspired by the report from Dr. Ing. Yves Wild Ingenieurbüro GmbH (2005), whereas the MGO price is based on Bergen Bunkers AS (2022).

The alternative cost of transportation can be challenging to estimate. We set this value to 100 000 NOK for ports where the passenger vessel service is the only realistic public transportation option, and 500 NOK if alternatives exist, such as a bus or car ferry connection.

The next cost parameter is the value of passenger time. We distinguish between passenger time spent waiting in port, and transit time spent on board. For the time spent on board, we use 112 NOK/h as estimated by Flügel et al. (2020). For the value of time spent waiting for a departure, Wardman et al. (2016) find that the waiting cost in a system with high frequency should be 1.5 times higher than the cost of time spent on board. In our test instances, however, the frequency is set substantially lower than in Wardman et al. (2016). Own observations have shown that in systems with low frequencies, the travelers plan ahead and arrive with a distribution skewed towards the departure time. We thus assume that the cost of waiting in port is reduced to 0.5 times the cost of time spent aboard, i.e., C^{PW} thus becomes 56 NOK/h.

The final cost parameters are the crew costs for each vessel type. These are calculated based on Tveter et al. (2020). We apply their costs of an eight-hour shift of 4 098 NOK and 2 727 NOK for senior and junior crew, respectively.

5.2. Test instances

We generate three different test instances by varying the ports included. They are named All Ports (AP), Near Ports (NP) and High Demand (HD). In the AP instance, the selection of ports is made as similar to the existing service as possible. In other words, we include all 20 ports in the Florø basin shown in Fig. 4. This test instance acts as the main instance in the subsequent analyses due to its comparability to the existing vessel service.

In the NP instance, we seek to construct a test case with shorter sailing distances. As all routes have Florø as a central hub, the ports are selected based on their distance from Florø. We define this test instance with Florø and the eight ports closest to Florø. The candidate frequencies are equal as in the AP test instance. The motivation for

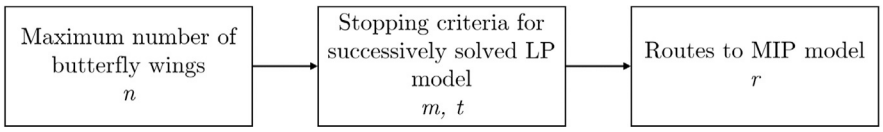

Fig. 5. Overview of parameters in the DB heuristic.

Table 2
Objective values in peak period and computational time for different values of m for performance test instance P2 (m is the maximum number of iterations without a new best solution from the LP model).

m	10	50	100	500	1000	10 000
Objective value in peak period	1 537 648	61 531	57 026	57 026	57 026	57 026
Time (s)	0.8	6.7	31	83	145	1 091
New best found	1	2	3	3	3	3

solving this instance is to analyze a service where a lower travel distance is covered as range is a key challenge with adoption of battery electric vessels.

Finally, in the HD instance, we only include the ports that have a passenger demand higher than the average value of the demand to and from Florø. This gives a test instance with eight ports, including Florø. The aim of solving this instance is to show the effects of a service with somewhat higher demand per port than the current service.

6. Computational results, analyses and managerial insights

The results from solving the test instances for zero emission and conventional vessels are presented in Sections 6.2 and 6.3. After presenting these results, we discuss three focal aspects of the solutions. In Section 6.4, we describe how replanning vessel services leads to improved adaption of zero emission operations. In Section 6.6, we perform sensitivity analyses of two important parameters, i.e., the electricity price and passenger cost of sailing. Finally, Section 6.7 discusses the implications of changes in the future carbon taxation levels and the effects of an increased carbon tax on abatement costs for the studied instances.

6.1. Parameter setting and performance evaluation for the DB heuristic

As outlined in Section 4, the DB heuristic consists of some parameters, summarized in Fig. 5, which need to be set to obtain as good performance as possible. In the following we present the process for setting these parameter values for the AP instance and the results thereof (although we followed a similar approach for the other two instances).

First, we test the number of wings to include in the route generation, n, where we test for $n = 1, 2, 3, 4$. Increasing the value of n significantly increases the number of routes and the computational time for generating these (c.f., Appendix B). When setting $n = 1$, we obtained no feasible rotations, meaning that none of the candidate ZE vessels are able to serve the whole set of ports in one round trip within the time period. When n is set to 4, we found that the number of routes and rotations became too large to be handled. Hence, we were left with $n = 2, 3$.

Furthermore, we vary the parameter m, which decides the maximum number of iterations without a new best solution from the LP model. Here, we set the time criterion, t, sufficiently high to make it redundant. Table 2 shows the objective value in the peak period when $n = 2$ for different values of m. In this case, 18 900 rotations are created and the time used for the first step of the DB heuristic, i.e., route generation, rotation generation and proxy evaluation and sorting, is only 80 s. The table also presents the time used successively solving the LP model (step 2 of the DB heuristic) and the number of times the current best solution is updated. Table 2 shows that when $m = 100$, we obtain the same objective value as for all higher values of m tested.

The same procedure is conducted for $n = 3$, where as many as 212 058 rotations are generated and the computational time of step 1 of the DB heuristic increases to 880 s. These results are summarized in Table 3.

By comparing the objective values in Tables 2 and 3, we see that $n = 3$ provides better solutions. Hence, routes consisting of three wings are better for the peak period, and we set $n = 3$. In the DB heuristic, the strategic decisions are determined with the aim of optimizing the objective value in the peak period. Accordingly, as discussed above, the parameter m must be set greater than or equal to 500, and we must allow for routes consisting of three wings, i.e., $n = 3$. Even though we want to minimize computational time, we also want the number of stored solutions to be of an appropriate size, increasing the probability of including routes better suited for the other time periods (i.e., in step 3). Accordingly, we set $m = 5000$. This gives a total computational time for steps 1 and 2 of 1 518 s (880 and 638 s in steps 1 and 2, respectively).

With n set to 3 and m set to 5000, we need to find an appropriate value for the parameter r for the MIP model constituting the final and third step of the DB heuristic. The r parameter determines the size of the set of available routes in each remaining time period. Here, we fix the strategic decisions from step 2, which also provides a set of stored rotations, sorted after their objective value for the peak period. Table 4 shows the objective values (now across all time periods) and the solution times for step 3 when the number of input routes r vary.

Table 4 shows that a higher number of routes yields, as expected, better solutions. This indicates that a good route in the peak period is not necessarily good in other time periods. It should be noted that the value of m bounds the value of r. Increasing m (most likely) leads to an increase in the number of routes, because more rotations, and consequently more routes are included in the stored solutions sent to the MIP model. In this case, the number of unique routes sent to the MIP model is cut off at a number lower than 320, which means that there is no use in increasing the value of r beyond 320 in this case. Hence, we set r at = 320, which yields an objective value of 153 202 for all time periods. The total computational time of the DB heuristic then accumulates to 2478 s for all three steps of the DB heuristic.

6.2. System costs breakdown and strategic decisions

In the following, we focus on the cost breakdown and the strategic decisions of the AP, NP and HD instances. To save space, we show a detailed cost breakdown only for the AP instance alongside associated optimal strategic decisions. The cost breakdown of the AP test instance is presented in Table 5. The zero emission (ZE) solution is denoted as AP−ZE, while the conventional solution is denoted as AP−C. Table 6 shows the optimal strategic decisions in AP−ZE and AP−C.

We observe from Table 5 that AP−ZE has around 30% higher costs than AP−C. This cost difference represents the abatement cost, i.e., the

Table 3
Objective values in peak period and computational time for different values of m for performance test instance P3, with the best values marked in bold (m is the maximum number of iterations without a new best solution from the LP model).

m	10	50	500	5 000	10 000	100 000
Objective value in peak period	55 508	55 508	**55 140**	**55 140**	**55 140**	**55 140**
Time (s)	0.7	3.6	64	638	1 251	20 350
New best found	1	2	2	2	2	2

Table 4
Objective value and computational time for different sizes of the set of candidate routes, r. The best objective value is indicated in bold.

r	5	10	20	40	80	160	320
Objective value	164 921	163 921	163 716	155 676	155 631	153 212	**153 202**
Time (s)	4.1	7.7	18.1	42	118	797	960

Table 5
Cost breakdown of the AP instance.

Cost term	AP-ZE		AP-C		
	Value (NOK)	% of total	Value (NOK)	% of total	% of ZE
Vessel investment	39 722	25.9%	19 861	16.6%	50.0%
Infrastructure investment	2 388	1.6%	*NA*	*NA*	*NA*
Energy cost	20 720	13.5%	26 984	22.6%	130%
Crew cost	38 208	24.9%	19 104	16.0%	50.0%
Cost of alt. transport	7 821	5.1%	10 318	8.6%	132%
Cost of unvisited ports	16	0.0%	16	0.0%	100%
Cost of waiting at port	32 776	21.4%	38 278	32.0%	117%
Transit cost	11 549	7.5%	4 912	4.1%	42.5%
Total system cost	153 202	100.0%	119 474	100.0%	78.0%

Table 6
Strategic decisions in the AP instance.

Decision	AP-ZE	AP-C
Vessel type	1M	1C
Total number of vessels	2	1
Infrastructure	Florø	–

Table 7
Abatement cost of the different instances.

Instance	ZE cost	Conventional cost	1 day	1 year	20 years
AP	153 202	119 474	33 728	12.3 mill.	246 mill.
NP	63 729	61 757	1 972	0.72 mill.	14.4 mill.
HD	149 659	111 922	37 737	13.8 mill.	276 mill.

cost of introducing an emission-free passenger vessel service. We further break the results into the terms of the objective function. The vessel investment costs in the ZE case are double those in the conventional case. This is caused by the acquisition of two vessels in the ZE case, as opposed to one in the conventional case. Furthermore, the charging infrastructure investment is naturally only applicable to the ZE case. Charging infrastructure is only installed in Florø, and the infrastructure costs constitute a low percentage of the total costs. The energy costs are substantially lower in the ZE case. This is closely linked with the operating speeds of the respective services. The ZE vessels operate at lower speeds along the sailing legs than the conventional vessels. The latter consequently consumes more energy, and the costs are higher as the unit cost of energy is almost the same for both technologies, as described in Section 5.1. The crew costs are also doubled in the ZE solution, which follows naturally from doubling the number of vessels.

Moving on to the cost of alternative transport, this is lower in AP-ZE. This is a result of the different routes chosen in the two situations, as illustrated in Fig. 6, which shows the chosen routes in time period 3 for (a) AP-ZE and (b) AP-C. The figure shows that the northernmost subroute is sailed twice in the ZE case due to having two vessels available, while it is only sailed once in the conventional case since only one vessel is available. Hence, more passengers are transported along the northernmost subroute by the ZE service than by the conventional one. Lower frequency also leads to a higher cost of waiting in port in AP-C. On average, the passengers using the conventional service wait longer in the ports than passengers using the ZE service. The cost of unvisited ports is negligible, because the demand is very low from and to the single port, Stavang (i.e., the most right port in the figures), which is excluded in both cases. A reason for this is that most ports of the Florø route are situated on islands where no alternative means of transportation exist. Finally, the transit cost is much higher for the ZE solution than the conventional one, which is caused by the lower sailing speeds.

The NP and HD instances yielded similar result, but the most notable difference is that for the NP instance, the cost difference between the ZE and conventional solution is significantly lower than for the AP and HD cases. This is mainly caused by lower costs incurred by vessel investments and crew, as only one vessel is needed to serve the route.

Summary of abatement costs for all instances

The abatement costs (in NOK) of transitioning to a ZE service are displayed in Table 7 for all instances. An interesting metric is the abatement cost per passenger. We make this calculation for the AP instance. The observed demand adds up to approximately 342 passengers per day. Thus, the daily abatement costs for a trip becomes $33\,728/342 \approx 100$ NOK/passenger.

6.3. Route and frequency decisions

This subsection investigates the differences in route and frequency decisions across the test instances and time periods.

Subroute configurations for ZE operations

The limited energy storage and reach of the ZE vessels is one reason for a choosing butterfly route where the vessel(s) can do charging in the hub (Florø) several times. The main reason for choosing a butterfly route with more than one subroute operated by different vessels (as shown in Fig. 6(a)), is the requirement of covering the route within

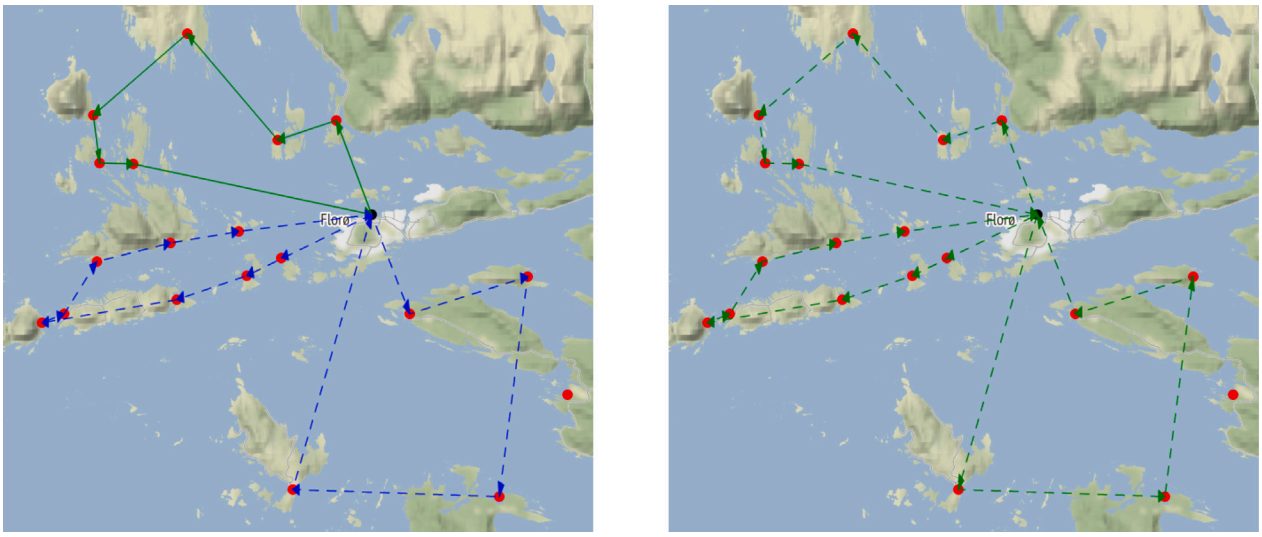

(a) AP-ZE: Subroutes operated in time period 3 (b) AP-C: Route operated in time period 3

Fig. 6. Route structures in time period 3 for (a) ZE vessels and (b) conventional vessels. Different colored lines indicate separate subroutes operated by different vessels. Dashed lines indicate a frequency of one, whereas solid lines indicate a frequency of two.

the time periods. Long (sub-)routes lead to both longer sailing times and increased charging times, which might not be feasible within the time periods. Therefore, the alternative is to split the routes into several subroutes operated by different vessels. This enables the service to visit the required ports, but also induces the acquisition of extra vessels and associated crew costs. Using the conventional solution as a baseline for solutions without charging requirements, we observe that the route adjustment comes at a cost. This cost is not sufficiently counteracted by the cost reductions of offering the passengers a better service, making the ZE-solutions the costlier alternative, as seen in Tables 5 and 7.

The best route structures of AP-ZE and AP-C for time period 3 (Fig. 6) exemplifies the above. Apart from an opposite sailing direction in the southern butterfly wing and a different service frequency in the northern wing, the only difference is a separation into two subroutes for the ZE vessel service, a consequence of the limitation with respect to time, mentioned above. Although incurring an extra cost, operating two subroutes rather than one enables increased frequency levels in subroutes where this outweighs the additional energy costs

How different demands affect the route choices

The demand vary over the four time periods of the day, and is significantly higher in periods 1 and 3, corresponding to morning and afternoon, respectively, since there are many commuters going to and from the main hub, Florø, in these periods. Fig. 7 shows the chosen routes for the AP-ZE test instance for time periods 1 (morning) and 4 (evening), where the evening time period has less than 30% of the demand of the morning period. Some major differences in the routes become apparent. First, the ports are served by a butterfly route with three wings (and two subroutes) in time period 1, whereas the route in time period 4 only has two wings and subroutes. In general, a higher total demand leads to more wings for ZE vessels. The second interesting observation is that the sailing direction of the southern butterfly subroute is changed between time periods 1 and 4. The direction is a result of minimizing the passenger costs by reducing average transit times in the subroute. The service frequency however, is a trade-off between the additional energy cost of sailing twice as long within the same time period, and the decreased passenger costs of waiting in port and the need for alternative transportation. This trade-off has resulted in different outcomes for the two time periods, with a frequency of two in the southern subroute in the high demand time period 1 in contrast to only one in time period 4.

We can also compare the routes in the AP-ZE for time period 1 (Fig. 7(a)) and time period 3 (Fig. 6(a)). Since these two periods are dominated by commuters going to Florø in period 1 and from Florø in period 3, we see that the chosen routes have opposite directions for the reasons discussed above. Otherwise, the routes are quite similar to each other, except for that there are different subroutes which get a higher frequency when operated by ZE vessels.

Ability to omit ports

So far, omitting ports has not been discussed thoroughly. We can observe from Figs. 6 that Stavang is the only port that is not visited in time period 3. Further, it is observed from Table 5 that skipping Stavang incurs a cost of just 16 NOK per day, implying that it costs more than 16 NOK to sail the detour to and from Stavang. Stavang is considered a mainland port, meaning that the cost of alternative modes of transportation is set to 500 NOK per passenger. For the island ports, there are no other options than to make use of the vessel service since the cost of alternative modes of transportation is set to 100 000 NOK per passenger, as described in Section 5.1. As a result, the island ports are only bypassed in periods when the demand at the island is zero, which can be observed in Fig. 7, where the port of Alvora is skipped.

By detaching from the real scenario and rather defining all ports as mainland ports, we can vary the cost of alternative transportation and inspect at which cost the different ports are visited. The result of this analysis is summarized in Fig. 8 for the AP-ZE instance, showing the number of ports visited in time period 3.

As Fig. 8 shows, the number of visited ports increases in the cost of alternative transportation, or vice versa, the number of omitted ports increases with decreased cost. The reasoning behind which new ports that are added in the routes as this cost increases is complex. One could presume that the ports with the highest demand would be included first. This is to some extent true, but it also depends on the distance from the already included ports. To exemplify, the inclusion of a port would in some cases only be feasible if the solution includes a larger vessel (or even an extra vessel) or an extra port with infrastructure.

6.4. Value of optimizing routes and frequency levels

To further analyze the value of optimizing routes and service frequency levels of ZE vessel services, we investigate ZE solutions where

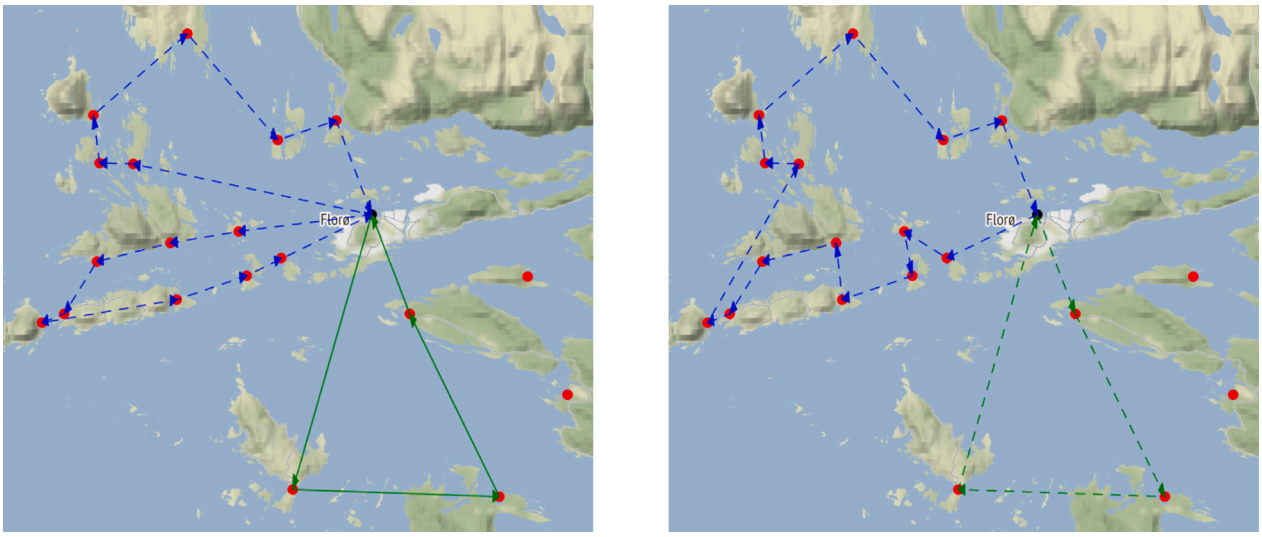

(a) AP-ZE: Subroutes operated in time period 1 (b) AP-ZE: Subroutes operated in time period 4

Fig. 7. Routes in AP-ZE for time periods 1 (a) and 4 (b). Different colored lines indicate separate subroutes operated by different vessels. Dashed lines indicate a frequency of one, whereas solid lines indicate a frequency of two.

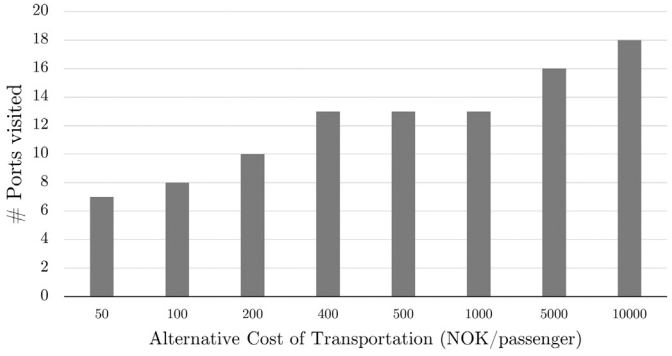

Fig. 8. Ports visited for different values of the cost of alternative transportation, C^{ALT}, in period 3.

the route and frequency levels are fixed to those in the best conventional solutions. The purpose is to showcase that route plans for existing vessels may no longer be appropriate with the adoption of ZE vessels. To make the results comparable, we create three additional test instances, AP-ZE-F, NP-ZE-F and HD-ZE-F, where the route structures and frequency levels are fixed, prior to solving, to their values in the best solutions found for AP-C, NP-C and HD-C, respectively. We first analyze the results from NP-ZE-F, which are summarized in Table 8. The fixation of the routes and frequency levels from the best conventional solution gives in total a cost increase of 2.4%, which gives an indication of the value of optimizing routes and frequencies. The vessel investments are higher as a different vessel type is acquired compared to the optimized service NP-ZE. In addition to a different vessel type, service frequencies are fixed to higher levels than for NP-ZE which result in a need for increased sailing speeds. Higher sailing speeds require more energy, thus increasing the energy cost substantially. The increased frequency levels in the NP-ZE-F compared to the NP-ZE also contribute to reductions in passenger costs, i.e., cost of alternative transportation, cost of waiting in port and transit cost, which mitigate some of the increase in operator costs.

The results for the AP-ZE-F and HD-ZE-F instances are also interesting, as these do not even have a feasible solution. This shows that transferring the route and frequency decisions from conventional vessels directly to ZE vessels is not possible. These two instances have longer sailing distances than the NP instance. To complete long routes within the four hour time periods, the conventional vessels must maintain a high speed, which sometimes can be problematic for ZE vessels. Higher speed implies a higher energy usage, again forcing longer charging times. Therefore, the AP-ZE-F and HD-ZE-F instances become infeasible because completing the routes and maintaining the frequency is impossible within the time period duration of four hours. In the AP-ZE and HD-ZE test instances (where the route and frequencies are optimized), this is solved by splitting the routes in two subroutes for each time period. The result that conventional services require replanning to be operated by ZE vessels is in line with Sundvor et al. (2021) who found that only 15% of the Norwegian high-speed passenger vessel services are suitable for battery-electric propulsion if maintaining their current pattern of operation.

6.5. Speed selection

The selection of sailing speeds affects multiple cost factors in the model, i.e., it directly affects passenger and energy cost, and it indirectly affects infrastructure cost (positioning of charging facilities) and vessel investment (battery size). An important observation is that the gain in passenger costs from increasing speeds is reduced by the need for additional charging for ZE vessels, while conventional vessels do not experience this, thus increasing the gain from sailing faster with conventional vessels. Hence, one could assume that the ZE vessels would sail slower for all comparable route legs to reduce power consumption, but as the ZE vessels need to finish sailing and charge their batteries within the length of each time period, they cannot select arbitrarily low speed levels. This effect sometimes causes the ZE vessels to sail faster than the conventional ones.

Another important observation is the variation in selected speed levels with varying passenger demand. We observe that due to the sailing speeds' effect on the passenger costs, sailing legs with few passengers onboard are often sailed at lower speeds and vice versa. Similarly, in time periods of high demand (e.g., peak-demand in the afternoon), the routes are often sailed faster than the time periods with fewer travelers. However, the factors explaining the speed levels are non-trivial and dependent on a wide range of other decision variables as well. We have pointed to several factors explaining the speed selection here, but decisions regarding whether a route is divided into multiple subroutes (and thus adding more vessels), their respective battery sizes,

Table 8
Cost breakdown of the NP-ZE-F test instance.

Cost term	NP-ZE-F		
	Value (NOK)	% Change from NP-ZE	% Change from NP-C
Vessel investment	19 861	7.4%	0.0%
Infrastructure investment	2 388	0.0%	–
Energy cost	11 310	206%	22.2%
Crew cost	19 104	0.0%	0.0%
Cost of alt. transport	5 978	−42.0%	0.0%
Cost of waiting in port	4 616	−39.7%	0.0%
Transit cost	1 993	−4.4%	−32.2%
Total system cost	65 250	2.4%	5.7%

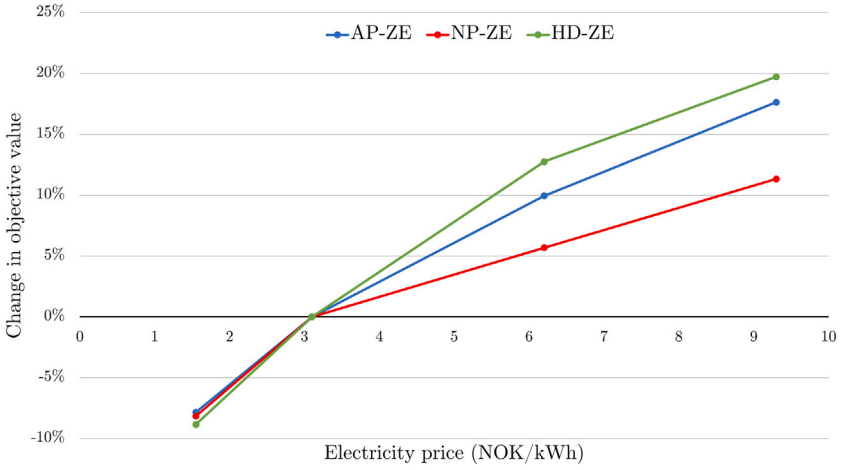

Fig. 9. Objective value change as a function of the electricity price.

and the placement of additional charging capacity would often lead to deviations from the "simple" answer that speed levels strictly follow the demand for transportation and vessel propulsion technology. In general, we see that sailing speeds in our solutions are selected across the entire range of available options (i.e., between 10 and 30 knots), with an average in the upper half of the range.

6.6. Sensitivity analyses

There are some cost parameters that are more uncertain that the others, e.g., the future price of electricity, defined by the parameter C^{VC}_{pi}, and the value of the passenger time, C^{SW}. In the following we perform sensitivity analyses with respect to these two cost parameters.

Electricity price

An electricity price of 3.1 NOK/kWh was assumed in our analyses so far (Section 5.1). Now, we run the model with three additional electricity prices for each test instance to see how sensitive the costs are to varying electricity prices, i.e., we test with prices that are 50%, 200% and 300% of the original ones. The relationship between total system cost (objective value) and electricity price is shown in Fig. 9 for each of the three test instances.

We observe from Fig. 9 that the HD−ZE instance is the most sensitive to changes in the electricity price. This is caused by a higher overall sailing speed than in the other instances. The best solutions with an increased electricity price is when sailing speed is reduced to lower the electric power consumption. When the sailing speed is reduced, the service is worsened for the passengers. This effect is weakest for the NP−ZE instance. This is due to the short sailing distances and low passenger demand, which again makes passenger costs less affected by increased electricity prices and reduced sailing speeds.

Passenger cost of sailing

In the following, we conduct a sensitivity analysis of the value of passenger time while sailing, C^{SW}. The analysis is performed also on the conventional test instances, since this cost parameter is equally relevant for both the conventional and ZE models. In Section 5.1, the cost parameter was set to 112 NOK/h. Now, we run the model with three parameter values for each instance to see how sensitive the costs are to varying passenger cost of sailing, i.e., we test with prices that are 50%, 200% and 300% of the original ones.

From the results shown in Fig. 10, one may observe that the ZE solutions are more sensitive to changes in the cost of sailing parameter, except for the NP instances. The difference between the NP instance and the other instances is that the transit cost constitutes a larger part of the objective value for NP−C than for NP−ZE.

When the cost parameter is reduced, the vessels in all instances sail slower. This causes a frequency reduction in most instances. The reduced frequency yields a worse service for the passenger and the unmet demand increases. In the peak period, the model seeks to uphold the frequency to reduce the amount of unmet demand. As the strategic decisions are based on the peak period (following how the heuristic solution method works, this could lead to worse solutions overall when the cost parameter is reduced, as observed for the HD−ZE instance. For the HD−ZE instance, a route structure consisting of two subroutes is chosen, where both subroutes are served with a frequency of two, at the original value of the cost parameter. When the cost parameter is reduced, so is the frequency in one of the subroutes, while a frequency of two is maintained in the other. In the subroute with a frequency of one, the vessel may reduce its speed, and hence a vessel with reduced battery capacity is chosen. Since the same vessel type must be used in all subroutes, infrastructure is installed in an extra port in the subroute with a service frequency of two, to maintain the required speed level. The extra infrastructure is not needed in the other time periods, since the vessels simply reduce their speed levels when the demand is lower.

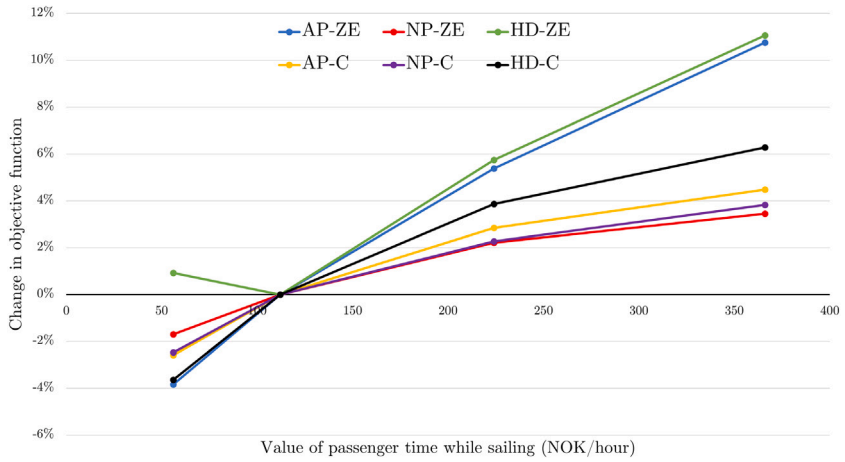

Fig. 10. Change in objective function value for different value of passenger time while sailing.

Table 9
Overview of daily CO_2-emissions in the different instances.

Instance	Fuel consumption (kg)	CO_2-emissions (kg)
AP-C	758.3	2426.6
NP-C	260.2	832.6
HD-C	905.3	2897.0

Thus, regardless of the reduction in the cost parameter, we obtain worse objective values overall in this instance.

6.7. Implications of carbon pricing

One important aspect of the choice between ZE and conventional energy carriers, is the environmental benefit of reduced CO_2-emissions. The taxation of CO_2-emissions has become an important political instrument, intending to reduce emissions (The World Bank, 2014). This aspect is not directly accounted for by the ZEVSNDP. We thus present an analysis of the emissions from the different test instances and the implications of a carbon taxation scheme for these instances. We calculate the CO_2-emissions based on the fuel consumption in the instances, and use a conversion rate of one kilogram fuel to 3.2 kilograms of CO_2 (Statistics Norway, 2017). Table 9 shows the daily fuel consumption and corresponding CO_2 emissions for each of the test instances with conventional vessels.

From Table 9, we observe that the fuel consumption, and consequently the CO_2-emissions, are far higher for instances AP−C and HD−C, than for NP−C. In the former instances, longer distances are covered, naturally yielding a higher consumption. Furthermore, HD−C is operated at higher speeds than AP−C, which accounts for the difference between these instances.

A measure of particular interest is the abatement costs of transitioning to a ZE service. The abatement costs describe the extra costs associated with transitioning from the best found conventional service to the best found ZE service. We further show the implications of different levels of CO_2-taxes for the abatement cost. The relationship between tax levels and abatement costs for instances AP−C and HD−C are shown in Fig. 11. The results for NP−C is presented on its own in Fig. 12 as the abatement costs are far lower than for the other two instances.

Note that instance HD−C has a steeper reduction in the abatement costs than instance AP−C when the tax increases. This is caused by higher emissions in this instance, making it more sensitive to changes in tax levels. The cost of the NP−C instance breaks even at a tax of 2 369 NOK/ton CO_2. Norwegian politicians and experts have expressed a goal of an emission taxation level of 2 000 NOK/ton by 2030 (Energi og Klima, 2021), and the break-even cost is thus not far from this goal in the NP instance. It is thus a highly interesting test instance when transitioning to ZE operations in the Florø basin.

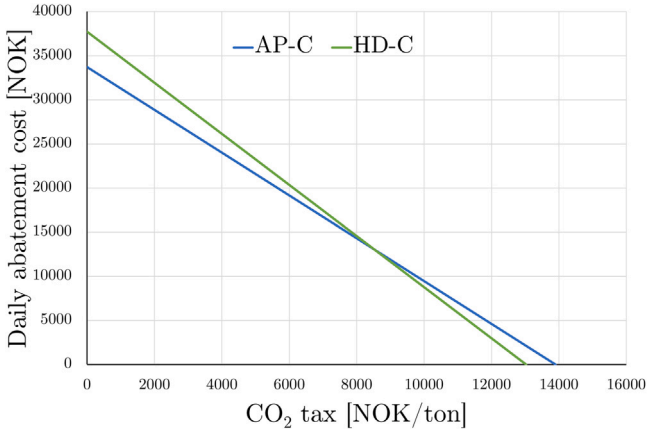

Fig. 11. Abatement cost for the AP and HD instance.

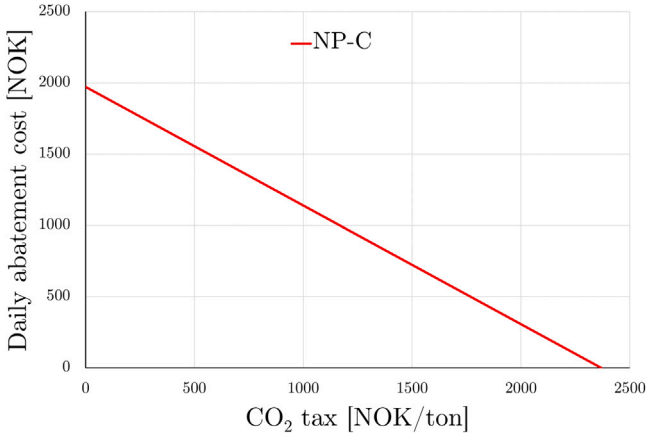

Fig. 12. Abatement cost for the NP instance.

Table 10 shows the break-even CO_2-tax level for all instances in the first row, while the abatement costs at the tax level of 2000 NOK/ton are shown in the second row. Finally, the third row presents the abatement costs with a tax level of 2000 NOK/ton, relative to a zero tax rate. Table 10 shows that a tax level of 2000 NOK/ton is insufficient

Table 10
Overview of the effect of a CO_2-tax on the different instances.

Instance	AD	NP	HD
Break-even CO_2-tax (NOK/ton)	13 899	2 369	13 026
Abatement cost at 2 000 NOK/ton (NOK)	28 875	307	31 943
% of original abatement cost	85.6%	15.6%	84.6%

for all instances, and for instances AD and HD in particular. However, if the tax level becomes higher, the NP test instance may be viable as a ZE alternative.

7. Conclusions

This paper has significantly extended the recent contribution by Havre et al. (2022) on optimal planning of zero emission high-speed vessels by accommodating joint assessment of routing and scheduling decisions for multiple planning periods with varying demands. This development provides new insights into cost-effective zero emission vessel operations, in particular by advising suitable route layout and emphasizing the role of substitute modes in minimizing transport costs.

Despite the added flexibility of route choice, the Florø case study analyzed using the ZEVSNDP supports the findings of Havre et al. (2022) that abatement costs for battery electric high-speed vessels substantially outweigh the Norwegian government's target for the social cost of carbon. A notable exception is the sub-case considering only ports in close proximity. In line with Sundvor et al. (2021), this suggests that only a fraction of existing connections that service short routes are likely to be viable for battery electric vessels. An important distinction is that Sundvor et al. (2021) analyze technical feasibility of *current operations*. This paper shows that route planning is an important tool for ensuring technical feasibility and that enabling battery electric maritime transport can require splitting existing routes into multiple sub-routes that are operated by individual vessels. Whilst adding substantial operator costs, our results show that such modification may benefit passengers by enabling higher frequency. This may in turn attract new travelers that can be especially beneficial in cases where it helps alleviating external costs of road transportation through mode shift. This is particularly relevant in the urban setting as costs related to road congestion is among the most significant externalities of road transport (Wangsness et al., 2020). This is an interesting avenue for further research that reaches beyond the scope of the current paper.

The ZEVSNDP gives novel insights into suitable route layout for a zero emission service. The computational study shows that a dynamic route structure that accommodates changes in demand over the course of the day is cost-effective. For the Florø case, adopting the *butterfly shape* enables a single charging hub while the number of wings are determined by time-of-day demand. This structure reduces the need for costly up-front investment in new energy systems, which are among main financial concerns of county councils in charge of providing public transport in Norway.

Changing current timetables is considered politically sensitive, and the aim of regional policy makers has consequently been to swap existing vessels without affecting level of service. The results of this study show that this strategy may not be technically feasible for battery electric vessels. In general, upholding existing timetables tailored to conventional vessels leads to *too high* service speed and thereby energy consumption of zero emission vessels. We therefore encourage decision makers to acknowledge changes in cost structure of vessel services from adoption of zero emission vessels to reap economic benefits from tailoring services to the characteristics of battery electric vessels.

Acknowledgments

The authors are grateful to the anonymous reviewers, whose comments helped us improve the paper. This paper is a part of the research project enabling Zero Emission passenger Vessel Services (ZEVS), funded by the Research Council of Norway (Grant no. 320659). The authors are indebted to the ZEVS's many user partners for their input. Support from the Institute for Energy Technology, the public transport agencies Ruter and Kolumbus, the shipbuilder Brødrene Aa, and Statkraft AS has been vital.

Appendix A. Summary of the notation for the zero emission model

Sets	
$\mathcal{P}$	Set of planning periods
$\mathcal{R}_p$	Set of potential routes in period p
$\mathcal{C}_r$	Set of subroutes in route r
$\mathcal{K}_c$	Set of legs in route c
$\mathcal{I}$	Set of all ports
$\mathcal{I}_c$	Set of ports in route c
$\mathcal{F}_c$	Set of potential frequencies in subroute c
$\mathcal{V}$	Set of available vessel types
$\mathcal{S}_v$	Set of discrete speed levels for vessel type v
Parameters	
$\overline{T}_p$	Length of planning period p
T_{prckvs}	Sailing time of leg k in subroute c in route r in period p with speed s and vessel type v
$\underline{T}_i^W$	Minimum waiting time in port i to allow passengers to enter and exit the vessel
T_{prckl}^U	Travel time from port at the beginning of leg k to port beginning at leg l in subroute c in route r in period p with the fastest vessel type available, sailing at its fastest speed level, with no charging or waiting time beyond the minimum requirements
W_{prcf}	Average waiting time at frequency f in time period p for subroute c in route r
D_{prckl}	Maximum demand from port at the beginning of leg k to port at the beginning of leg l in subroute c in period p with route r
D_{prcklf}	Demand from port at the beginning of leg k to port at the beginning of leg l in subroute c in period p with route r at frequency f
Q_v	Passenger capacity of vessel type v
E_{prckvs}	Energy consumption on leg k in subroute c in route r in period p with vessel type v sailing at speed s
$\overline{B}_v$	Maximum battery level of vessel type v
$\underline{B}_v$	Minimum battery level of vessel type v
$\overline{P}_i$	Available charging power in port i
A_{prcik}	1 if leg k starts at port i in subroute c in route r in period p, 0 otherwise
C_v^{FC}	Fixed cost per vessel of type v
C_i^{INF}	Fixed cost of investing in charging infrastructure in port i
C_v^{crew}	Crew cost of using vessel v for one hour
C_{pi}^{VC}	Cost per unit of energy charged in port i in period p
C_{pr}^{ALT1}	Alternative cost per passenger not transported due to unvisited ports in route r in period p
C_{prckl}^{ALT2}	Alternative cost per passenger not transported between port at the beginning of leg k to port at the beginning of leg l in subroute c in route r in period p
C^{PW}	Value of passenger time while waiting at port
C^{SW}	Value of passenger time while sailing
Variables	
α_i	1 if charging infrastructure is built in port i, 0 otherwise
δ_v	1 if vessel type v is chosen, 0 otherwise
y_v	Number of vessels of type v bought

β_{pr}	1 if route r is chosen in period p
g_{prcv}	Number of vessel v used in subroute c in route r in period p
z_{prcf}	1 if frequency f is chosen for subroute c and route r in period p, 0 otherwise
$x_{prckvfs}$	Weight variable for speed s for vessels of type v on leg k in subroute c in route r served with frequency f in period p
l_{prcklv}	Number of passengers traversing leg k with destination port at the end of leg l in subroute c with a vessels of type v in route r in period p
$q_{prcklvf}$	Number of passengers picked up in port at the beginning of leg k with destination at the port in the beginning of leg l in subroute c with route r in period p with frequency f with vessel type v
u_{prckl}	Unmet demand between port at the beginning of leg k and port at the beginning of leg l in subroute c with route r in period p
t^{RT}_{prcvf}	Total round trip time in subroute c for a vessel of type v with route r served with frequency f in period p
$c_{prcikvf}$	Charging time in port i before traversing leg k in subroute c served with frequency f with a vessel of type v in route r in period p
$w_{prcikvf}$	Time spent in port i before sailing leg k in subroute c when served with frequency f with a vessel of type v in route r in period p
t_{prckl}	Transit time from port at the beginning of leg k to port at the beginning of leg l in subroute c in route r in period p
b_{prckv}	Battery level when starting on leg k for vessels of type v in subroute c route r in period p

Appendix B. Heuristic route generation

The heuristic route generation first constructs a set of main routes. Then, all possible configurations of subroutes are generated for each main route. The two separate generation methods are explained in detail in the following.

Generation of main routes

The route generation proposed as a part of the DB heuristic produces both cyclical and butterfly routes, as these two structures resemble the routes found in the area of our case study today, and are thus assumed to be found reasonable. The butterfly routes, in particular, are interesting on account of three characteristics: (1) They result in, on average, shorter travel times to a central hub, which is very relevant for our case study where many are traveling to and from the port of Florø. (2) Butterfly routes allow for multiple subroute configurations. A different number of vessels and varying frequencies in the different subroutes enable a more customized transport system. (3) Butterfly routes reduce the need for charging infrastructure. By visiting a port several times throughout a route, vessels can utilize the infrastructure (if installed in the hub), more than once through their route, and thus reduce the need for investments in charging capabilities. For simplicity, the cyclical routes generated in this method are referred to as (butterfly) routes with one wing. We generate the main routes through the following five steps:

1. Divide the ports into n natural groups based on geographical locations/regions. All groups of ports should be mutually exclusive, except one port, the central hub (Florø in our case study), that should appear in all of them.
2. Based on the groups from the previous step, create butterfly routes with up to n wings. For a butterfly route with n wings, each port group becomes a separate wing. However, for butterfly routes with a lower number of wings, groups must be combined to create the correct wings.
3. Within each wing, we solve a Traveling Salesman Problem (TSP), and organize the ports in order to minimize total travel distance in the wing. The TSP is solved using a Miller–Tucker–Zemlin formulation, as described by Miller et al. (1960).

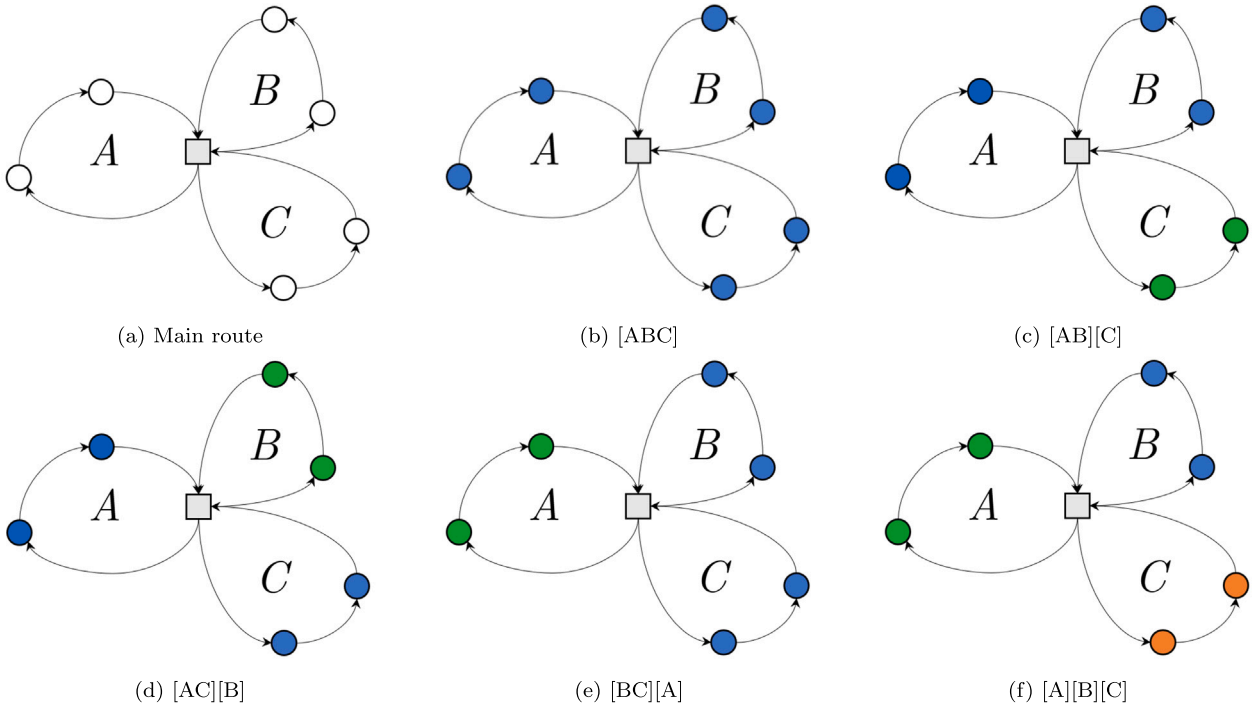

Fig. B.1. Main butterfly route and its possible subroute configurations.

4. The routes created this far have not considered the different directions a wing may be sailed, e.g., clockwise or counterclockwise. To account for this, we copy each route and generate a new route with the opposite direction.
5. The final step of the route generation is removal of ports. Up to this point, all routes contain all ports, combined in a unique fashion. The process, performed on every route, proceeds as follows: Make a copy of the route, and remove the port with the lowest alternative cost induced by not visiting it. This cost is the product of demand and the alternative cost of transportation per passenger demanding travel to or from the port. Continue this process until a predefined number of ports remain.

Configuration of subroutes

The division of routes into subroutes is straightforward. For each generated butterfly route, all possible divisions into subroutes are generated. To illustrate the process, consider a butterfly route consisting of three wings as illustrated in Fig. B.1(a). For a butterfly route with three wings there exists five possible configurations of subroutes. One option is to let all wings be the same subroute, as illustrated in Fig. B.1(b), denoted [ABC]. Further, there are three ways of separating three wings into two subroutes, [AB][C], [AC][B] and [BC][A], shown in Fig. B.1(c)-e. The last subroute configuration available, is a configuration where all wings are placed in different subroutes, [A][B][C], as presented in Fig. B.1(f).

The generation of all subroute configurations is performed for every main route. After this process, a route is distinguished from another not only by its sequence of ports, but also by its underlying subroute configuration. The set of routes is now complete, containing a diverse set of cyclical and butterfly routes, with a broad specter of subroute configurations. These routes are subsequently passed on to the next step of the DB heuristic, the generation of rotations.

References

Andersson, H., Fagerholt, K., & Hobbesland, K. (2015). Integrated maritime fleet deployment and speed optimization: Case study from RoRo shipping. *Computers & Operations Research*, *55*, 233–240.

Arbex, R. O., & da Cunha, C. B. (2015). Efficient transit network design and frequencies setting multi-objective optimization by alternating objective genetic algorithm. *Transportation Research, Part B (Methodological)*, *81*, 355–376.

Aslaksen, I. E., Svanberg, E., Fagerholt, K., Johnsen, L. C., & Meisel, F. (2020). Ferry service network design for kiel fjord. *Lecture Notes in Computer Science*, *12433 LNCS*, 36–51.

Aslaksen, I. E., Svanberg, E., Fagerholt, K., Johnsen, L. C., & Meisel, F. (2021). A combined dial-a-ride and fixed schedule ferry service for coastal cities. *Transportation Research Part A: Policy and Practice*, *153*, 306–325.

Bergen Bunkers AS (2022). Daily market update. URL https://www.bergenbunkers.no/wp-content/uploads/2022/05/pdf-markets-11.pdf.

Brouer, B. D., Alvarez, J. F., Plum, C. E. M., Pisinger, D., & Sigurd, M. M. (2014). A base integer programming model and benchmark suite for liner-shipping network design. *Transportation Science*, *48*(2), 281–312.

Buba, A. T., & Lee, L. S. (2019). Hybrid differential evolution-particle swarm optimization algorithm for multiobjective urban transit network design problem with homogeneous buses. *Mathematical Problems in Engineering*, *2019*, 1–16.

Dr. Ing. Yves Wild Ingenieurbüro GmbH (2005). Determination of energy cost of electrical energy on board sea-going vessels. URL http://www.effship.com/PartnerArea/MiscPresentations/Dr_Wild_Report.pdf.

Energi og Klima (2021). Klimameldingen: Varsler kraftig Økning i CO_2-avgiften. URL https://energiogklima.no/nyhet/dette-vet-vi-om-innholdet-i-regjeringens-klimamelding/.

EU (2021). *Second annual MRV report on CO2 emissions from maritime transport covering 2019 emissions*. European Union.

Fagerholt, K., Laporte, G., & Norstad, I. (2010). Reducing fuel emissions by optimizing speed on shipping routes. *Journal of the Operational Research Society*, *61*(3), 523–529.

Flügel, S., Halse, A. H., Hulleberg, N., Jordbakke, G. N., Veisten, K., Sundfør, H. B., & Kouwenhoven, M. (2020). Verdsetting av reisetid og tidsavhengige faktorer. Dokumentasjonsrapport til Verdsettingsstudien 2018–2019 (in Norwegian). *Institute of Transport Economics*, *1762*.

Grzelakowski, A. S., Herdzik, J., & Skiba, S. (2022). Maritime shipping decarbonization: Roadmap to meet zero-emission target in shipping as a link in the global supply chains. *Energies*, *15*, 6150.

Havre, H. F., Lien, U., Ness, M. M., Fagerholt, K., & Rødseth, K. L (2022). Cost-effective planning and abatement costs of battery electric passenger vessel services. *Transportation Research Part D: Transport and Environment*, *113*, Article 103495.

IMO (2020). *Fourth IMO GHG study 2020*. International Maritime Organization.

Klier, M. J., & Haase, K. (2015). Urban public transit network optimization with flexible demand. *OR Spectrum*, *37*(1), 195–215.

Kontovas, C. A. (2014). The green ship routing and scheduling problem (GSRSP): A conceptual approach. *Transportation Research Part D: Transport and Environment*, *31*, 61–69.

Lai, M. F., & Lo, H. K. (2004). Ferry service network design: optimal fleet size, routing, and scheduling. *Transportation Research Part A: Policy and Practice*, *38*(4), 305–328.

Liu, Y., Feng, X., Yang, Y., Ruan, Z., Zhang, L., & Li, K. (2022). Solving urban electric transit network problem by integrating Pareto artificial fish swarm algorithm and genetic algorithm. *Journal of Intelligent Transportation Systems: Technology, Planning, and Operations*, *26*(3), 253–268.

McKinlay, C. J., Turnock, S. R., & Hudson, D. A. (2021). Route to zero emission shipping: Hydrogen, ammonia or methanol? *International Journal of Hydrocarbon Engineering*, *55*, 28282–28297.

Miller, C. E., Tucker, A. W., & Zemlin, R. A. (1960). Integer programming formulation of traveling salesman problems. *Journal of the ACM*, *7*(4), 326–329.

Reusser, C. A., & Osses, J. R. P. (2021). Challenges for zero-emissions ship. *Journal of Marine Science and Engineering*, *9*, 1042.

Rinaldi, M., Parisi, F., Laskaris, G., D'Ariano, A., & Viti, F. (2018). Optimal dispatching of electric and hybrid buses subject to scheduling and charging constraints. In *IEEE conference on intelligent transportation systems, proceedings, ITSC. 2018-November* (pp. 41–46).

Ritari, A., Spoof-Tuomi, K., Huotari, J., Niemi, S., & Tammi, K. (2021). Emission abatement technology selection, routing and speed optimization of hybrid ships. *Journal of Marine Science and Engineering*, *9*(9).

Rogge, M., van der Hurk, E., Larsen, A., & Sauer, D. U. (2018). Electric bus fleet size and mix problem with optimization of charging infrastructure. *Applied Energy*, *211*, 282–295.

Sassi, O., & Oulamara, A. (2017). Electric vehicle scheduling and optimal charging problem: Complexity, exact and heuristic approaches. *International Journal of Production Research*, *55*(03), 519–535.

Shang, H., Liu, Y., Huang, H., & Guo, R. (2019). Vehicle scheduling optimization considering the passenger waiting cost. *Journal of Advanced Transportation*, *2019*.

Statistics Norway (2017). Emission factors used in the estimations of emissions from combustion. URL https://www.ssb.no/_attachment/291696/binary/95503?_version=547186.

Sundvor, I., Thorne, R. J., Danebergs, J., Aarskog, F., & Weber, C. (2021). Estimating the replacement potential of norwegian high-speed passenger vessels with zero-emission solutions. *Transportation Research Part D: Transport and Environment*, *99*, Article 103019.

The World Bank (2014). Pricing carbon. URL https://www.worldbank.org/en/programs/pricing-carbon.

Thun, K., Andersson, H., & Christiansen, M. (2017). Analyzing complex service structures in liner shipping network design. *Flexible Services and Manufacturing Journal*, *29*(3), 535–552.

Totten, J. C., & Levinson, D. M. (2016). Cross-elasticities in frequencies and ridership for urban local routes. *Journal of Public Transportation*, *19*(3), 117–125.

Tveter, E., Rødseth, K. L., Hoff, K., Rødal, J., & Thune-Larsen, H. (2020). Forslag til nye kriterier for båter i inntektssystemet for fylkeskommunene (in Norwegian). *Møreforskning Molde AS*, *24*, 90.

Villa, D., Montoya, A., & Herrera, A. M. (2020). The electric riverboat charging station location problem. *Journal of Advanced Transportation*.

Wangsness, P. B., Proost, S., & Rødseth, K. L. (2020). Vehicle choices and urban transport externalities. Are Norwegian policy makers getting it right? *Transportation Research Part D: Transport and Environment*, *86*, Article 102384.

Wardman, M. (2001). A review of british evidence on time and service quality valuation. *Transportation Research Part E: Logistics and Transportation Review*, *37*, 107–128.

Wardman, M., Chintakayala, V. P. K., & G., de Jong (2016). Values of travel time in Europe: Review and meta-analysis. *Transportation Research Part A: Policy and Practice*, *94*, 93–111.

Zhang, L., Zeng, Z., & Gao, K. (2021). Optimal design of mixed charging station for electric transit with joint consideration of normal charging and fast charging. *Smart Innovation, Systems and Technologies*, *231*, 85–94.